Outlook

Your manuscript has been accepted for publication: JBI-25-0188

De Journal of Biogeography <jbioffice@wiley.com>
Data Seg, 21/07/2025 06:21
Para Thiago Sanna Freire Silva <thiago.sf.silva@stir.ac.uk>
Cc Diego Pereira Santos <diegopsantos@live.com>; Fábio Afonso Mazzei Moura de Assis Figueiredo <figueiredo.uema@gmail.com>

WILEY

Dear Dr. Thiago Sanna Freire Silva,

We are delighted to inform you that your manuscript "CLIMATE CHANGE MAY INCREASE ENVIRONMENTAL SUITABILITY OF THE BABASSU COMPLEX (Attalea spp., ARECACEAE)" has been accepted for publication in Journal of Biogeography.

You can find reviewer comments at the bottom of this email, if applicable.

What happens now?

We will now check that all of your files are complete before passing them to our production team for processing. We will let you know soon if we require any further information.

Once the manuscript has been sent to production, Wiley will email the corresponding author with information about:

- Signing the license
- Paying any applicable article publication charges (APCs)
- Reviewing manuscript proofs

To learn more, read Wiley's publication guide for authors.

If your submission contains supporting information, please read Wiley's supporting information FAQs. Supporting information is not copyedited, checked, or changed from its original format. If you notice an error, please get in touch with us as soon as possible.

Thank you for choosing to publish with Journal of Biogeography.

MANUSCRIPT DETAILS

Kind regards,
Journal of Biogeography

P.S. – You can help your research get the attention it deserves! Wiley Editing Services offers professional video abstract and infographic creation to help you promote your research. You can also read Wiley's free Promotion Guide for best-practice recommendations on effectively promoting your work.

Reviewer comments:

> "
>
> ***Reviewer 1 Comments to the Author***
>
> > *Thank you for addressing the previously suggested comments. I am*

satisfied with the current version of the manuscript, which shows great improvements compared to the previous one. However, I would like to share two additional points that I believe could contribute to the final refinement of the text:

1. Lines 164–165: "The predictor variables used to model the current climate scenario covered the reference period from 2011 to 2040."
I was left with a question regarding the choice of this reference period to represent the current climate conditions. Could you clarify why the 2011–2040 interval was used instead of 1981–2010? Referring to 2011–2040 may generate some confusion, as it is still an ongoing period and could, in some contexts, be interpreted as part of a future scenario. As I understand it, the CHELSA baseline data refer to the period 1979–2013 (Karger et al. 2017), so including a brief justification in the manuscript might help clarify this methodological decision.

2. Regarding data analysis and representation.
I understand the choice of a descriptive approach in the comparison between climate scenarios, based on the visual interpretation of the maps. However, considering that there are methodologies available for statistically comparing cell values across different scenarios (see Silva et al. 2024), I suggest that statements regarding the variation (increase or decrease) in suitable areas be presented with caution, given the absence of statistical validation. It remains as a suggestion for future research.

References
Karger, D., Conrad, O., Böhner, J. et al. Climatologies at high resolution for the earth's land surface areas. Sci Data 4, 170122 (2017). https://doi.org/10.1038/sdata.2017.122
Silva, A.S.S., Arnan, X. & de Medeiros, P.M. (2024). Climate change may affect the availability of wild food plants in the Brazilian semiarid region. Regional Environmental Change 24, 86. https://doi.org/10.1007/s10113-024-02250-3

I congratulate the authors on the progress made and wish you success with the publication.

Reviewer 2 Comments to the Author

I would like to express my appreciation to the authors for their thorough responses, as all my concerns have been adequately addressed.

CLIMATE CHANGE MAY INCREASE ENVIRONMENTAL SUITABILITY OF THE BABASSU COMPLEX (*Attalea spp.,* ARECACEAE)

Diego Pereira Santos

Programa de Pós-Graduacão em Biodiversidade e Biotecnologia da Amazonia Legal, Universidade Estadual do Maranhão (UEMA), São Luís, Maranhão, Brazil, diegopsantos@live.com, https://orcid.org/0000-0003-4967-8245

Thiago Sanna Freire Silva

Division of Biological and Environmental Sciences, Faculty of Natural Sciences, University of Stirling, Stirling, Scotland, UK, thiago.sf.silva@stir.ac.uk, https://orcid.org/0000-0001-8174-0489

Fábio Afonso Mazzei Moura de Assis Figueiredo

Departamento de Zootecnia, Universidade Estadual do Maranhão (UEMA), São Luís, Maranhão, Brazil, figueiredo.uema@gmail.com, https://orcid.org/0000-0002-6904-9828

Acknowledgements

The authors wish to thank the Programa de Pós-Graduação da Rede Amazônica em Biodiversidade e Biotecnologia (BIONORTE), the Fundação de Amparo à Pesquisa e ao Desenvolvimento Científico e Tecnológico do Maranhão (FAPEMA), the Brazilian Federal Foundation for Support and Evaluation of Graduate Education (CAPES), the University of Stirling and the State University of Maranhão (UEMA), especially the Laboratory of Environmental Sciences and Biodiversity (LCAB/UEMA), for their financial and operational support of this study, and to the reviewers who provided their expertise in evaluating this manuscript. No new fieldwork was conducted for this study, all occurrence data were obtained from publicly accessible databases (GBIF), and all bioclimatic variables were sourced from the CHELSA database. Therefore, no field permits were required.

Author contribution

D.P. Santos was responsible for compiling the database, conducting the modelling procedures, analysing the results, and preparing the figures and tables, under the guidance of the co-authors. All authors contributed to the conceptualization, writing, and revision of the manuscript.

Funding

This work was supported by the Fundação de Amparo à Pesquisa e ao Desenvolvimento Científico e Tecnológico do Maranhão (FAPEMA) (IECT-05539/18) and the Brazilian Federal Foundation for Support and Evaluation of Graduate Education (CAPES) (PDSE - 88881.846679/2023-01).

Conflict of Interest

The authors declare that there is no conflict of interest.

Biosketch

The authors operate at the intersection of forest ecology, conservation, and environmental modelling. Their collective expertise includes forest resources, silviculture, ecophysiology, and ecological modelling, with a strong focus on understanding species distribution, ecosystem dynamics, and responses to climate change. The team combines field-based research with geospatial analysis, remote sensing, and machine learning to explore patterns of biodiversity and ecosystem function.

CLIMATE CHANGE MAY INCREASE ENVIRONMENTAL SUITABILITY OF THE BABASSU COMPLEX (*Attalea spp.,* ARECACEAE)

CLIMATE CHANGE AND BABASSU PALM SUITABILITY

Abstract

Aim

This study aimed to identify the key bioclimatic factors driving the distribution of the Babassu Complex across the Neotropics in current scenario (2011-2040), and to project their range shifts under future climate scenarios (2041-2070 and 2070-2100).

Taxon

Babassu Complex (Arecaceae): *Attalea barreirensis*, *A. eichleri*, *A. funifera*, *A. maripa*, *A. phalerata*, *A. speciosa*, and *A. vitrivir*.

Location

Neotropical region.

Methods

We employed Species Distribution Modelling using four algorithms: Maximum Entropy (MaxEnt), Random Forest (RF), Boosted Regression Trees (BRT), and Generalized Linear Models (GLM) for the seven babassu species and for the combined Babassu Complex dataset. GBIF presence-only data was combined with CHELSA 2.1 bioclimatic variables from current and future scenarios to fit the models. Projections for 2041–2070 and 2071–2100 were derived for two high-emission climate scenarios (SSP3 7.0 and SSP5 8.5), using an ensemble of five global climate models.

Results

The RF and BRT algorithms provided more conservative predictions for the current scenario, while MaxEnt and GLM projected broader distributions. Temperature seasonality was the most important suitability predictor. *Attalea maripa*, *A. phalerata*, and *A. speciosa* showed broadest suitability ranges, while *A. funifera* and *A. vitrivir* were most constrained. Future scenarios projected major suitability increases (up to 871.80% for the Complex under SSP5-8.5 by 2071-2100), particularly in Amazonian and Cerrado regions. Only *A. funifera* and *A. vitrivir* showed declines (-8.55% and -20.97% respectively under SSP3-7.0).

Main conclusions

We anticipate that climate change may favour babassu species that tolerate warmer and more variable conditions, promoting their expansion. While this may support restoration and livelihoods, unmanaged spread could disrupt local ecosystems. It is recommended that future research focus on incorporating anthropogenic variables, validating

predictions with field data, and exploring species-specific ecological responses to climate change.

Keywords: Species Distribution Modelling (SDM); Habitat Suitability; Tropical Forests; Bioclimatic Predictors; Ecological Forecasting; Neotropical Palm; Babaçu.

INTRODUCTION

The Arecaceae family represents one of the largest and most ecologically significant tropical botanical families, contributing with the nutrients cycling, providing habitat structure, food, and materials for both biodiversity and local communities (Eiserhardt et al., 2011). Within this family, the genus *Attalea* is recognised as a major component of the Neotropical flora (Freitas et al., 2016; Pintaud, 2008). From the c.a. 40 species in the genus, at least seven recognised species and two hybrids form the "Babassu Complex": *Attalea barreirensis* Glassman, *A. eichleri* (Drude) A.J. Hend, *A. funifera*, *A. maripa* (Aubrl) Mart., *A. phalerata* Mart. ex Spreng., *A. speciosa* Mart. ex Spreng., *A. vitrivir*, *A. x teixeirana* (Bondar) Zona (a hybrid of *A. eichleri* and *A. speciosa*), and *A.* × *dahlgreniana* (Bondar) Wess. Boer (a hybrid of *A. speciosa* and *A. maripa*). Known locally as "babassu" or "babaçu," these palms are predominantly found in tropical countries such as Brazil, Mexico, Bolivia, Colombia, and Suriname (Teixeira 2008; Santos-Filho, Almeida Júnior, Soares 2013; Silva et al. 2014; Reis et al. 2018).

The Babassu Complex refers to a group of closely related *Attalea* species that exhibit overlapping morphological traits, frequent natural hybridization, and unresolved taxonomic boundaries (Cavallari & Toledo, 2016; Mata et al., 2022; Pintaud, 2008). Although its species share many anatomical features such as uniseriate epidermis, glandular scars, and dorsiventral mesophyll, they also show diagnostic differences in traits like stomatal distribution, vascular bundle organization, and palisade parenchyma layers (Mata et al., 2022), justifying their recognition as distinct taxa and supporting species-level ecological assessment.

From an ecological perspective, babassu palms are foundational species that influence forest structure, microclimate regulation, nutrient cycling, and soil stabilization across various Neotropical biomes (see Araújo et al., 2016; Corrêa et al., 2023; Porro, 2019; Ressiore C. et al., 2024). Socioeconomically, they support the livelihoods of traditional communities (Almeida Campos et al., 2015; Lima et al., 2003), such as the communities of babassu coconut breakers, women who rely on artisanal harvesting and

processing of its fruit given their broad range of uses (De Oliveira et al., 2022; Mitja et al., 2019; Porro et al., 2011; Shiraishi Neto, 2017), . These species can be utilised for handicrafts, construction, and human consumption. The babassu species provide a diverse range of products, the babassu nuts are the most prominent, which have the potential to be processed into various by-products with different levels of processing complexity, including mesocarp flour (Cardoso Vieira et al., 2023), oil (Neto et al., 2021), adsorptive material for chemical molecules (Vieira et al., 2011), biofuel, charcoal (Corrêa et al., 2023), and animal feed (Portela et al., 2024).

Comprehension of the ecological dynamics and distribution patterns of babassu is, therefore, imperative to ensure the sustainability of such socio-ecological systems and to support conservation and spatial planning efforts across the Neotropics. Climatic variables are especially relevant for palms, whose distributions are often closely tied to thermal and moisture regimes (De Kort et al., 2021; Eiserhardt et al., 2011; Peterson et al., 2011). While variables such as water availability and temperature seasonality are recognized as key determinants for many tropical palms (Kissling et al., 2012) the specific climatic thresholds that shape the distribution of babassu species remain unresolved.

As a powerful tool in conservation biogeography, the emergence of Species Distribution Modelling (SDM) has been instrumental in bridging knowledge gaps related to the geographic distribution of species and identifying species–climate relationships (Elith & Franklin, 2013; Guisan & Thuiller, 2005; Guisan & Zimmermann, 2000), encompassing historical biogeography, diversity patterns, ecosystem conservation, and the impacts of climate change (Brun et al., 2020; Franklin, 2023; Freer et al., 2018; Maltby et al., 2020; Volis & Tojibaev, 2021). The employment of advanced SDM techniques, involving bioclimatic variables and multiple algorithms, furnishes valuable insights into species distributions and potential niche shifts under prevailing and future climate scenarios (Alves et al., 2019; Brun et al., 2020; Katuwal et al., 2023; Valavi et al., 2022). This is of particular importance for palms and its pivotal ecological roles in tropical ecosystems and economical importance for local communities (Blach-Overgaard et al., 2010; Costa et al., 2022; Mitja et al., 2019).

Previous SDM studies have assessed the climatic suitability of *Attalea* species. Menezes et al. (2023) projected future distributions of *A. pindobassu* in the Brazilian biome Caatinga under the scenarios SSP2-4.5 and SSP5-8.5, finding drastic losses of suitable habitat, especially under pessimistic scenarios. Likewise, De Lima et

al. (2022) modelled 15 palm species in the Atlantic Forest, including *A. dubia* (Mart.) Burret and *A. humilis* Mart. Ex Spreng., revealing conservation gaps and spatial mismatches between suitable habitats and protected areas. However, no comprehensive multi-species SDM has been conducted for the Babassu Complex. These previous efforts have either focused on single species or specific regions, limiting their relevance for broader-scale conservation and land-use planning, what represents a critical gap. The lack of spatially explicit, climate-based assessments at the group level hinders our ability to anticipate range shifts, identify conservation priorities, and develop adaptation strategies under climate change.

Given their ecological dominance, socioeconomic importance, and biogeographic significance, the Babassu Complex is a high-priority group for climate impact assessments. Thus, the objective of this study is to identify the key bioclimatic factors driving the distribution of the Babassu Complex and its species across the Neotropical region, and project their range shifts under future climate scenarios (SSP3-7.0 and SSP5-8.5) across two periods (2041–2070 and 2071–2100), thereby contributing to a more nuanced understanding of their vulnerability and resilience in a changing climate.

MATERIAL AND METHODS

Data Collection

This study focused on species distribution modelling (SDM) for the seven species of the *Attalea* genus identified as part of the Babassu Complex and for the combined dataset. The species selection was based on their taxonomic inclusion in the Babassu Complex, supported by anatomical and morphological evidence (Cavallari & Toledo, 2016; Mata et al., 2022), the availability of sufficient georeferenced occurrence data for ecological modelling, and their ecological and socioeconomic importance across the region. Presence-only occurrence data were obtained from the Global Biodiversity Information Facility (GBIF) database, totalling 19,204 records distributed among species as follows: *A. phalerata* (n = 15,170), *A. maripa* (n = 3,580), *A. eichleri* (n = 142), *A. speciosa* (n = 129), *A. funifera* (n = 84), *A. barreirensis* (n = 52), and *A. vitrivir* (n = 47) (Figure 1).

To minimise spatial sampling bias, duplicate and spatially clustered, occurrences were filtered from the dataset so that only one occurrence per 20 km grid cell

was retained. This filtering procedure was used to reduce the influence of highly sampled cluster, often associated with accessible or well-surveyed areas, while preserving broader landscape-level occurrence patterns (Lake et al., 2020; Lee et al., 2022). After filtering, the number of retained occurrence points per species was: *A. barreirensis* (n = 41), *A. eichleri* (n = 79), *A. funifera* (n = 65), *A. maripa* (n = 570), *A. phalerata* (n = 431), *A. speciosa* (n = 84), *A. vitrivir* (n = 27), and the combined dataset (n = 1,269).

Bioclimatic Variables

For both current and future scenarios, bioclimatic variables were sourced from the Climatologies at High Resolution for the Earth's Land Surface Areas (CHELSA) database, version 2.1 (Table S1.2), which incorporates orographic corrections (e.g. wind fields, valley exposure) to enhance the accuracy of temperature and precipitation estimates in complex terrains (Brun et al., 2022; Karger et al., 2017, 2020, 2021). Each variable was obtained as a georeferenced TIFF file (GeoTIFF) with an original resolution of 30 arc-second (~1 km^2), using a geographic coordinate system referenced to the WGS 84 horizontal datum.

The predictor variables employed to model the current climate scenario covered the baseline period of 2011-2040. For future scenarios, the bioclimatic predictors were obtained from the *Scenario Model Intercomparison Project* (SMI), part of the *Coupled Model Intercomparison Project Phase 6* (CMIP6), accessed via the CHELSA V2.1 database. We considered two Shared Socioeconomic Pathways (SSPs) of high greenhouse gas emission: SSP3 7.0 and SSP5 8.5, and two time periods: 2041–2070 and 2071–2100. These scenarios were chosen to represent upper-bound climate change trajectories relevant for ecological risk assessments and stress-testing conservation planning. While recent studies have questioned the global plausibility of SSP5-8.5 due to evolving energy and policy trends (Hausfather & Peters, 2020; Scafetta, 2023), both SSP3-7.0 and SSP5-8.5 remain valuable for identifying potential biodiversity impacts in regions where mitigation policies are less consistent or delayed, such as parts of the Neotropics. SSP3-7.0 assumes a fragmented world with low international cooperation, while SSP5-8.5 represents a fossil-fueled development trajectory with high energy demand (Riahi et al., 2017). In this context, these scenarios were not used as predictions, but as boundary conditions to explore the vulnerability and resilience of the Babassu

Complex under contrasting high-risk futures. The projections were based on all five Global Climate Models (GCMs) available in the CHELSA database: National Oceanic and Atmospheric Administration - Geophysical Fluid Dynamics Laboratory (GFDL-ESM4), Met Office Hadley Centre (UKESM1-0-LL), Max Planck Institute for Meteorology (MPI-ESM1-2-HR), Institut Pierre Simon Laplace (IPSL-CM6A-LR), and Meteorological Research Institute (MRI-ESM2-0).

Pre-processing and modelling

The occurrence of palms has been primarily observed in tropical regions (Eiserhardt et al., 2011); moreover, the distribution of babassu species appears to be centred in the Neotropics (Teixeira 2008; Santos-Filho, Almeida Júnior, Soares 2013; Silva et al. 2014; Reis et al. 2018). Thus, all models were generated for the Neotropical region, encompassing Central and South America and the Caribbean. The SDMs were implemented using an integration of the sdm (Naimi & Araújo, 2016) and dismo (Hijman et al., 2024) packages in R 4.3.2. The models were trained using 70% of the retained occurrence points, with the remaining 30% being allocated for model testing.

Species distribution models based on presence-only data rely on recorded occurrences and do not account for confirmed absences. To compensate, researchers have employed various strategies to refine model predictions and improve ecological inference, such as the use of background points (Renner et al., 2015). To minimise sampling bias and acted as 'pseudo-absence' data in the models, ten thousand background points were randomly generated across the Neotropical region, which corresponds to the biogeographic extent of the Babassu Complex and reflects the broad ecological amplitude of the *Attalea* genus. This number is frequently recommended in SDMs studies to ensure sufficient environmental coverage while maintaining computational efficiency (Radomski et al., 2022; Valavi et al., 2022; Whitford et al., 2024) . The selection of background points in SDMs varies considerably (Steen et al., 2024; Whitford et al., 2024), and it is well known that using large background extents can inflate environmental gradients and potentially compromise model realism, particularly for species with narrow distributions and few occurrence records (Vasquez et al., 2021). In our case, species such as *A. vitrivir* (n = 27) and *A. barreirensis* (n = 41) are restricted in space (see Figure 1), which could increase sensitivity to this issue. However, because no detailed information exists on their climatic tolerances or dispersal constraints, defining a more ecologically

precise background would be speculative. As such, the Neotropical background was retained for all species to maintain consistency and support comparative and ensemble analyses. Moreover, benchmark studies show that presence-background models can still achieve reliable performance for rare species, provided that background points are well-distributed and model complexity is appropriately managed (Valavi et al., 2022; Whitford et al., 2024). Our approach thus seeks to balance ecological realism and methodological consistency, while acknowledging the limitations of modelling poorly known and geographically restricted species.

Multicollinearity is a common issue in ecological modelling, as it complicates the estimation of variable effects and reduces model extrapolation accuracy (Brun et al., 2020; Graham, 2003). To address this, a multicollinearity analysis was conducted (Dormann et al., 2013), for the seven species and Babassu Complex overall using all the bioclimatic variables considered for constructing the bioclimatic models. Variance inflation factors (VIF) were calculated using the *vifstep* function from the *usdm* package (Naimi et al., 2014), utilising default specifications, with variables showing VIF > 10 considered highly collinear and excluded to prevent overfitting.

Given the unavailability of evapotranspiration and vapour pressure deficit data for future climate scenarios in the CHELSA database, a correlation analysis was conducted utilising Spearman's coefficient (See Figure S1.1) on the complete set of current bioclimatic variables. This analysis, performed with the *rcorr* function from the *Hmisc* package (Hijman et al., 2024), identified the most strongly correlated variables to substitute for missing predictors. To avoid redundancy, each missing predictor was replaced only by its single most correlated variable, ensuring that a given predictor was not associated with multiple replacements. All the remaining predictors used for current and future scenarios can be found in Table S1.3. For the current scenario, multicollinearity analysis resulted in 8 to 12 variables being kept in model formulations. The most frequently retained predictors included mean diurnal temperature range (MDTR), mean monthly precipitation amount of the warmest quarter (MMPAWaQ), mean daily mean air temperatures of the wettest quarter (MDTWeQ), and precipitation amount of the wettest month (PAWM), which appeared in at least seven of the eight models (Figure S1.2). Conversely, annual precipitation amount (APA) (*A. speciosa* model), mean monthly potential evapotranspiration (PPMean) (*A. eichleri* model), mean monthly vapour pressure deficit (VPDMean) (*A. funifera* model), and mean daily mean air temperatures

of driest quarter (MDTDQ) (*A. maripa* and *A. phalerata* models) were less frequently selected.

To generate the SDMs for all the datasets in current and future scenarios, models were implemented using the sdm package, employing four algorithms with complementary modelling approaches: Boosted Regression Trees (BRT) (Friedman, 2001), Generalised Linear Models (GLM) (McCullagh & Nelder, 1989), Maximum Entropy (MaxEnt) (Phillips et al., 2006) and Random Forest (RF) (Breiman, 2001). These algorithms were chosen because they represent a diverse spectrum of statistical and machine learning methods, ranging from parametric (GLM), semi-parametric (MaxEnt), to non-parametric (BRT, RF), and are widely benchmarked in ecological niche modelling (Norberg et al., 2019; Qiao et al., 2019; Shabani et al., 2016). This diversity helps capture varying species–environment relationships while mitigating algorithm-specific biases in ensemble predictions (Valavi et al., 2022). To evaluate the mean performance of the algorithms, the k-fold cross-validation technique was implemented through the sdm function from the sdm R package. In this process, the occurrence data were divided into five folds, and the cross-validation procedure was repeated five times. This approach yielded 25 models (5 folds × 5 repetitions) per species–algorithm combination, thereby providing a robust assessment of model performance, utilising multiple random partitions as opposed to a single one (Phillips et al., 2006). The performance of the models was evaluated using the receiver operating characteristic (ROC) curve (Phillips et al., 2006), assessed based on area under the curve (AUC) values (Swets, 1988), True Skill Statistics (TSS) (Allouche et al., 2006), and deviance measures. AUC or TSS values of 1 indicate perfect predictive performance, while values of ≤ 0.5 suggest random prediction (Allouche et al., 2006; Swets, 1988). According to these metrics, all models showed good performance (AUC: 0.95–1.00; TSS: 0.85–0.99; Deviance: 0.08–0.37; Table S1.4a-c).

To assess the contribution of individual variables to the presence-absence of Babassu Complex species, we calculated relative variable importance (IR%), based on the mean AUC metric as implemented in the R package sdm (Naimi & Araújo, 2016). These values were then visualised using the *getVarImp* function. Both model performance metrics and IR% values are available in the metadata of the SDM objects.

Habitat suitability and presence-absence maps

Habitat suitability maps were generated for each of the four modelling algorithms (MaxEnt, RF, GLM, and BRT), for each individual species and for the Babassu Complex overall, using the predict function from the dismo package. For the current scenario (2011-2040), an ensemble suitability map was created by integrating the outputs from the four algorithms using a weighted average based on TSS performance criteria (Boali et al., 2024; Marmion et al., 2009). This ensemble approach balance interpretability and predictive power, following best practices for ecological forecasting, and ensures that better-performing models contribute more heavily to the final prediction (Valavi et al., 2022). For the future scenarios (2041-2070 and 2071-2100) under both SSP3-7.0 and SSP5-8.5, the ensemble suitability maps for each species and the Babassu Complex were generated by combining all individual model outputs (i.e. all four algorithms across each of the five GCMs) into a single ensemble per scenario for period, using TSS-weighted averages. All GCMs (GFDL-ESM4, UKESM1-0-LL, MPI-ESM1-2-HR, IPSL-CM6A-LR, and MRI-ESM2-0) were given equal representation, but individual model contributions were weighted by algorithmic performance (TSS). This method reflects ensemble modelling practices recommended for ecological forecasting under climate change, helps mitigate model-specific biases and offers a pragmatic balance between robustness and interpretability (Brun et al., 2020).

The resulting ensemble habitat suitability map for all scenarios were then transformed into binary presence-absence maps, delineating the potential distribution of the seven individual species and the Babassu Complex. This was achieved using the maximum thresholding method (maxSSS), which optimises the trade-off between sensitivity (true positive rate) and specificity (false positive rate) and is not affected by the use of pseudo absences (Liu et al., 2013).

Finally, the ensemble maps for both current and future scenarios were reprojected to a Universal Transverse Mercator (UTM) coordinate system and resampled to a spatial resolution of 1 km to allow area calculations, and to assess the change in suitable area between classes across scenarios. The suitability maps were classified into four categories: unsuitable (suitability ≤ 0.05), low suitability ($0.05 <$ suitability ≤ 0.33), medium suitability ($0.33 <$ suitability ≤ 0.66), and high suitability (suitability > 0.66). The cutoff for unsuitability corresponds to the lower 5th percentile of predicted suitability values, excluding areas environmentally equivalent to background conditions (Almpanidou et al., 2016; Liu et al., 2013). The thresholds for low and medium suitability follow widely used ENM classifications and represent a gradient of environmental

favourability (Jiménez-Valverde, 2014). Low suitability includes marginal habitats, often corresponding to the lower quantiles of predicted suitability (Liu et al., 2013; Sillero, 2011), while medium suitability includes suboptimal but viable environments for species persistence, consistent with transitional habitat categories in SDM frameworks (Franklin, 2010). High suitability reflects optimal conditions, defined here as the upper tercile (>0.66) of predictions based on robust threshold-selection methods (Liu et al., 2016), and aligning with core climatic niches in Neotropical species distributions (Costa et al., 2022). For the current scenario, area calculations were conducted independently for each of the following algorithms: BRT, GLM, MaxEnt, and RF, in addition to the ensemble map. For future scenarios, area calculations were performed for each emission scenario (SSP3 7.0 and SSP5 8.5) across distinct periods (2041–2070 and 2071–2100) for the ensembles only. A detailed methodological workflow is provided in a flowchart (See Figure S1.3). All image processing and map generation were conducted using QGIS Desktop 3.18.2 and R 4.3.2.

RESULTS

Relative Importance of Variables

Most variables demonstrated low importance across the majority of SDMs and models (Table 1.5a-h). Results varied significantly among SDMs, resulting in high standard deviations in the mean importance per predictor (n=100) and, consequently, high coefficients of variation. The highest mean Im% values were observed for GLM, while the lowest were found for RF.

Among all predictors, temperature seasonality (TS) emerged most frequently as the variable with the highest Im%, showing a notable association with the distribution of *A. barreirensis* (53.0%), *A. eichleri* (43.6%), *A. maripa* (20.6%), and the Babassu Complex overall (34.5%). Furthermore, *A. eichleri* exhibited robust responses to annual range of monthly vapour pressure deficit (VPDrange) and mean monthly vapour pressure deficit (VPDmean), *A. speciosa* to Isothermality (Iso), and *A. vitrivir* to minimum monthly potential evapotranspiration (PPmin) and precipitation amount of the driest month (PADM).

Predicted Current Habitat Suitability and Potential Distribution of the Babassu Complex

The spatial distribution of habitat suitability areas was found to be consistent across SDM predictions (Figure 4a-h), with variations primarily observed in suitability levels (Table S1.6). The GLM algorithm identified the largest areas of high habitat suitability across models (See Table S1.7), while BRT predicted the smallest high-suitability areas but the most extensive low-suitability regions, with a maximum suitability value of approximately 0.53. RF and BRT models had the most conservative estimates of habitat suitability for the babassu species, while MaxEnt and GLM projected broader areas in the medium and high suitability classes.

Among species, *Attalea speciosa* and *A. maripa* had the largest high-suitability areas, covering 927,503 km² and 915,496 km², respectively. Conversely, *A. vitrivir* (14,502,398 km²) and *A. funifera* (14,020,351 km²) had the most extensive unsuitable areas. For the Babassu Complex as a whole, the most extensive suitability class was medium suitability, covering 7,891,228 km².

Changes in habitat suitability in future climatic change emissions scenarios

The application of SDMs has revealed notable differences in the bioclimatic suitability of species from the Babassu Complex under current climate conditions, which has demonstrated significant adaptability across tropical regions of the Americas and the Caribbean, particularly in the Amazon rainforest and Cerrado (Figure 2a-h). At the species level, *A. barreirensis* and *A. eichleri* predominantly occupied savanna regions, including the Brazilian Cerrado and the Venezuelan Llanos. *A. funifera* exhibited the most restricted distribution, mainly within the tropical and subtropical moist broadleaf forests of the Brazilian Atlantic Forest, coastal Bahia, and the Brazil-Paraguay border, as well as parts of the tropical and subtropical dry broadleaf forests of the Caribbean and Central America. *A. maripa* showed an intrinsic relationship with the Amazon rainforest in northern South America. *A. phalerata* was found in tropical and subtropical moist forests, flooded grasslands of the Chaco and Pantanal, and savanna regions. Of all the species, *A. speciosa* demonstrated the largest potential distribution, encompassing transitional zones between the Cerrado and Amazon, adjacent areas, and savanna regions across the Americas (Cerrado, Llanos) and the Caribbean. Finally, *A. vitrivir* exhibited one of the smallest

distribution areas, being confined to the Brazilian Cerrado and the transition zones between the Cerrado, Caatinga, and Atlantic Forest.

The analysis revealed that the prediction maps generated by each of the algorithms, and when averaged together, indicated the Babassu Complex as having extensive potential to support its presence across South America. The areas of highest environmental suitability were found to be predominantly concentrated in the northwestern regions of the continent, significantly overlapping the Amazon rainforest. However, a substantial portion of these suitable areas was also identified within the Cerrado biome, indicating a potential intrinsic relationship with both ecosystems.

Comparison of habitat suitability areas between current and future scenarios (see Table 1 and Figure S1.4) indicate a substantial increase in high-suitability areas for most models and climate change scenarios, with the only reductions being observed in the 2071-2100/SSP3 scenario for *A. funifera* (-8.55%) and *A. vitrivir* (-20.97%). The scenario with the most significant increase in high-suitability areas for the majority of models was 2041-2070/SSP3 (Figure 3). For the Babassu Complex, the largest increases in high-suitability areas were recorded across all future scenarios, ranging from 680.78% in 2041-2070/SSP3 to 871.80% in 2071-2100/SSP5.

DISCUSSION

The selection of specific predictors, as observed for annual precipitation amount (APA) (*A. speciosa*), mean evapotranspiration (PPMean) (*A. eichleri*), mean vapour pression deficit (VPDMean) (*A. funifera*), and mean daily temperature in the driest quarter MDTDQ (*A. maripa* and *A. phalerata*), may indicate more species-specific environmental preferences (Brun et al., 2020; Dormann et al., 2013; Graham, 2003). However, it is important to note that the retention of these predictors does not necessarily imply a direct ecological response (Graham, 2003), underscoring the need for complementary field and physiological studies to validate these predictors' ecological significance.

The Relative Variable Importance (Im%) values demonstrated that humidity-related variables were not the most influential in modelling Babassu Complex distributions. Instead, temperature seasonality (TS), defined as the standard deviation of mean monthly temperature, exhibited a high retention frequency across species after multicollinearity removal and had the highest Im% values, identifying it as a key

predictor. These results corroborate Eiserhardt et al. (2011), who emphasized palm species' sensitivity to cold and seasonal climates due to limited frost tolerance and dormancy mechanisms These findings serve to reinforce the notion of the pronounced temperature sensitivity exhibited by palms and their marked preference for tropical climates (Eiserhardt et al., 2011).

Concerning SDMs, Generalised Linear Models (GLMs) have been shown to assign higher Im% values to individual bioclimatic variables in comparison to alternative modelling methods. In the context of GLMs, the occurrence of species is assumed to be associated with environmental variables according to a predefined relationship, thereby placing greater emphasis on variables that exhibit strong statistical associations. This sensitivity may result in an overemphasis on certain predictors, potentially reducing the reliability of species distribution projections and highlighting the importance of ensemble models (Hao et al., 2019; Marmion et al., 2009; McCullagh & Nelder, 1989). Conversely, Random Forest (RF) assigned lower numerical importance to individual predictors. This is because RF is a non-parametric algorithm based on an ensemble of decision trees, which distributes variable importance across multiple trees (Antoniadis et al., 2021; Breiman, 2001; Zhang et al., 2019). Consequently, RF tends to yield more balanced variable importance values, which are often lower than those observed in parametric models such as GLMs.

The broad suitability ranges exhibited by *Attalea maripa*, *A. phalerata*, and *A. speciosa* suggested high levels of tolerance to present-day bioclimatic conditions, which highlights the necessity for their management. In contrast, the more limited suitability zones of *A. funifera* and *A. vitrivir*, particularly the latter, indicating higher vulnerability to environmental fluctuations. This emphasises the necessity for the formulation of targeted conservation strategies to ensure the continued viability of these species in the context of climate change (Elliott et al., 2024; Lannuzel et al., 2021; Volis & Tojibaev, 2021). The use of a uniform Neotropical background extent for all species, including range-restricted taxa like *A. funifera*, *A. barreirensis*, and *A. vitrivir*, ensured methodological consistency and allowed comparative ensemble modelling. However, this approach may overestimate bioclimatic suitability for narrowly distributed species by incorporating ecologically irrelevant areas. While justified by limited ecological information on these species, future studies should explore species-specific extents based on dispersal capacity and biogeographic context to refine predictions (Vasquez et al., 2021; Whitford et al., 2024).

The variations observed among models in the current scenario are indicative of the inherent characteristics of the algorithms used, thus reinforcing the necessity for complementary approaches to enhance projection robustness and minimise methodological uncertainties. These differences arise from the way each algorithm processes environmental information. RF and BRT likely emphasised strong environmental signals and interactions within the training data, constraining their projections to regions with highly suitable conditions while prioritising complexity and precision (Antoniadis et al., 2021; Breiman, 2001; Friedman, 2001; Zhang et al., 2019). Conversely, MaxEnt and GLM, with their broader statistical assumptions, projected larger continuous areas of medium to high suitability, potentially incorporating marginally suitable regions (Guisan & Zimmermann, 2000; McCullagh & Nelder, 1989; Phillips et al., 2006).

Furthermore, the ensemble modelling framework combined parametric (GLM), semi-parametric (MaxEnt), and non-parametric (BRT, RF) algorithms to leverage complementary strengths: GLMs provided interpretable relationships between predictors and responses but often produced inflated variable importance values due to model assumptions, while machine-learning methods captured complex interactions and generalized more conservatively (Norberg et al., 2019; Valavi et al., 2022). Ensemble models mitigated individual algorithm biases, improving robustness, predictive reliability, and generalization capacity, particularly when dealing with species that have varied ecological traits and data availability (e.g., widespread generalists like *A. speciosa* vs. narrowly distributed taxa like *A. vitrivir*) (Hao et al., 2019; Kaky et al., 2020; Marmion et al., 2009; Valavi et al., 2022).

It is anticipated that climate change will favour species capable of tolerating warmer and more variable climatic conditions, thereby enhancing their performance and facilitating their spread into new areas (Blois et al., 2013). Projections indicate a potential expansion of bioclimatic suitability for species of the Babassu Complex under future climate scenarios. This expansion could significantly affect savanna ecosystems such as the Brazilian Cerrado and the Venezuelan Llanos, as well as degraded areas of the Amazon rainforest (Santos et al., 2022), potentially altering ecological dynamics and species interactions (Rosenblatt & Schmitz, 2014). The presence of highly suitable habitats in these regions may allow babassu species to disperse from adjacent ecosystems and integrate into local communities (Blois et al., 2013; Gehring et al., 2020).

This ecological shift presents both opportunities and risks. On one hand, babassu expansion may support biodiversity restoration and the livelihoods of traditional communities that depend on palm products (Mitja et al., 2019; Porro et al., 2011). On the other, unmanaged expansion could lead to ecological imbalances and potential invasiveness with the potential to reshape local vegetation structure, alter resource availability for other plants and animals, and influence key ecological processes such as fire regimes and competition for space and nutrients (Alves et al., 2019; De Kort et al., 2021; Gehring et al., 2020). This dual nature calls for proactive management strategies that mitigate ecological risks while maximizing socioeconomic and environmental gains through sustainable extractivism, agroforestry integration, and community-led conservation.

Despite potential ecological concerns related to mismanagement, Babassu palms are deeply integrated into the cultural and economic fabric of traditional communities, contributing with food, oil, fiber, and income (De Oliveira et al., 2022; Mitja et al., 2019; Porro et al., 2011; Shiraishi Neto, 2017). The projected expansion of climatically suitable areas for babassu species offers practical opportunities for both conservation and sustainable use of its species. Regions such as the Cerrado-Amazon transition zone and the Venezuelan Llanos, where species like *A. speciosa*, *A. maripa*, and *A. phalerata* are projected to expand, should be prioritized for sustainable extractivism and community-based agroforestry initiatives that align with traditional livelihoods and promote biodiversity conservation (Almeida Campos et al., 2015; De Oliveira et al., 2022; Mitja et al., 2019). In contrast, species with more restricted distributions and higher vulnerability to climatic shifts, including *A. vitrivir* and *A. funifera*, demand targeted in situ conservation actions in regions identified as future climatic refugia (Lannuzel et al., 2021; Volis & Tojibaev, 2021). Integrating species distribution models with local ecological knowledge and land-use planning offers a pathway for designing resilient socioecological systems that support both biodiversity and human well-being under climate change (Porro et al., 2011; Valavi et al., 2022).

Moreover, while SDMs predict broad future suitability, actual expansion is contingent on factors like dispersal ability, landscape connectivity, and biogeographic barriers. Thus, expansion is not guaranteed and must be interpreted with caution. These results also corroborate Eiserhardt et al. (2011), who emphasized palm species' sensitivity to cold and seasonal climates due to limited frost tolerance and dormancy mechanisms. This physiological sensitivity helps explain the concentration of unsuitable habitats in

arid and colder regions, where thermal stress and low humidity act as constraints on distribution.

Ongoing changes in land use and land cover have already had an impact on the geographic distribution of many species, disrupting taxonomic flows and reducing biodiversity at both present and future scales (Adhikari et al., 2022; Bellard et al., 2012; Trautmann, 2018). Given that some babassu species are associated with anthropized landscapes (Gehring et al., 2020; Santos et al., 2022), incorporating anthropogenic variables such as land use, biological interactions, topography, and edaphic conditions into modelling efforts could improve the accuracy of distribution projections (Blach-Overgaard et al., 2010; Frans et al., 2022; Nuñez-Penichet et al., 2024; G. C. Silva et al., 2023; Vedel-Sørensen et al., 2013; Zuquim et al., 2023). The resilience of these species to disturbed environments (Santos et al., 2022), coupled with the interaction of ecological and anthropogenic factors, may be key determinants of their persistence and potential expansion under future scenarios.

Moreover, it is imperative to interpret SDM predictions as testable hypotheses rather than as direct substitutes for actual population parameters. To ensure reliability and applicability in ecological planning, it is essential to validate these models when utilising them to guide conservation decisions (Lee-Yaw et al., 2022).

Research Limitations

While this study provides valuable insights into the climate-driven distribution shifts of the Babassu Complex, several limitations should be acknowledged. First, the use of a uniform Neotropical background extent for all species, including those with restricted distributions (e.g., *A. funifera*, *A. vitrivir*), may have overestimated suitability for rare taxa by incorporating ecologically irrelevant areas. Future studies could refine predictions by testing species-specific extents based on dispersal constraints or biogeographic barriers (Vasquez et al., 2021; Whitford et al., 2024). Second, anthropogenic factors such as land-use change, habitat fragmentation, and human-mediated dispersal were not incorporated, potentially inflating projected suitability in heavily modified landscapes (Blach-Overgaard et al., 2010; Nuñez-Penichet et al., 2024). Third, the models assume unlimited dispersal, ignoring geographic barriers (e.g., deforestation, mountain ranges) that may limit range shifts (Adhikari et al., 2022; Qiao et al., 2019). Finally, while ensemble modelling mitigated algorithmic biases, field

validation is needed to confirm predicted expansions, particularly for species with low occurrence records (Franklin, 2023; Lee-Yaw et al., 2022). Addressing these limitations through integrated socio-ecological frameworks will enhance the practical utility of SDMs for conservation planning.

CONCLUSIONS

The projected responses of Babassu species to climate change reveal distinct ecological strategies and potential biogeographic shifts. Generalist species such as *A. speciosa*, *A. maripa*, and *A. phalerata* show broad tolerance to warmer and more seasonal climates, suggesting potential range expansions into transitional and anthropized environments. In contrast, *A. vitrivir* and *A. funifera* show narrow climatic suitability, indicating higher sensibility to climate changes. These patterns underscore the dual role of climate as both a driver of expansion and a constraint on persistence, emphasizing the need for species-specific conservation strategies. Beyond mapping distributions, these findings contribute to a broader understanding of how tropical plant species may reorganize in response to shifting climatic envelopes. Such reorganization has implications not only for local ecosystems and community structure but also for long-distance floristic connectivity, endemism patterns, and the future configuration of Neotropical biotas.

By integrating the strengths of multiple algorithms and mitigating individual model biases, species distribution modelling (SDM) techniques provide robust insights into current and future biogeographic patterns. Within the Babassu Complex, these approaches have helped fill critical knowledge gaps, highlighting how species with different ecological traits and climatic tolerances may respond unevenly to environmental change. While ensemble species distribution models remain powerful tools for anticipating these changes, the key insight lies in their ecological interpretation: predicting not just where species might go, but how they will interact with existing communities and processes when they arrive.

A forward-looking conservation biogeography should therefore combine modelling with field validation and ecological data to better anticipate species responses. Thus, future research should focus on incorporating anthropogenic variables, validating predictions with field data, and exploring species-specific ecological responses to climate change. A multidisciplinary approach that combines species distribution modelling with

ecological and socioeconomic assessments will be essential for developing effective conservation and management strategies in the face of ongoing environmental change.

Data Availability Statement

All species occurrence records are available via GBIF, and bioclimatic variables were sourced from the CHELSA database. The full set of modelling scripts and processed data has been deposited on Zenodo (https://doi.org/10.5281/zenodo.15265496), ensuring full transparency and reproducibility of all analyses and results.

References

Adhikari, P., Kim, B.-J., Hong, S.-H., & Lee, D.-H. (2022). Climate change induced habitat expansion of nutria (Myocastor coypus) in South Korea. *Scientific Reports*, *12*(1), 3300. https://doi.org/10.1038/s41598-022-07347-5

Allouche, O., Tsoar, A., & Kadmon, R. (2006). Assessing the accuracy of species distribution models: Prevalence, kappa and the true skill statistic (TSS). *Journal of Applied Ecology*, *43*(6), 1223–1232. https://doi.org/10.1111/j.1365-2664.2006.01214.x

Almeida Campos, J. L., Da Silva, T. L. L., Albuquerque, U. P., Peroni, N., & Lima Araújo, E. (2015). Knowledge, Use, and Management of the Babassu Palm (*Attalea speciosa* Mart. Ex Spreng) in the Araripe Region (Northeastern Brazil). *Economic Botany*, *69*(3), 240–250. https://doi.org/10.1007/s12231-015-9315-x

Almpanidou, V., Schofield, G., Kallimanis, A. S., Türkozan, O., Hays, G. C., & Mazaris, A. D. (2016). Using climatic suitability thresholds to identify past, present and future population viability. *Ecological Indicators*, *71*, 551–556. https://doi.org/10.1016/j.ecolind.2016.07.038

612 Alves, C., Sousa-Silva, R., Marcos, B., Georges, D., & Lomba, A. (2019). Hoping the
613 best, expecting the worst: Forecasting the potential impacts of climate and land-
614 use change on Iberian plants of conservation concern. *Plant Ecology & Diversity*,
615 *12*(5), 507–518. https://doi.org/10.1080/17550874.2019.1641756
616 Antoniadis, A., Lambert-Lacroix, S., & Poggi, J.-M. (2021). Random forests for global
617 sensitivity analysis: A selective review. *Reliability Engineering & System Safety*,
618 *206*, 107312. https://doi.org/10.1016/j.ress.2020.107312
619 Araújo, F. R., González-Pérez, S. E., Lopes, M. A., & Viégas, I. D. J. M. (2016).
620 Ethnobotany of babassu palm (*Attalea speciosa* Mart.) in the Tucuruí Lake
621 Protected Areas Mosaic—Eastern Amazon. *Acta Botanica Brasilica*, *30*(2), 193–
622 204. https://doi.org/10.1590/0102-33062015abb0290
623 Bellard, C., Bertelsmeier, C., Leadley, P., Thuiller, W., & Courchamp, F. (2012). Impacts
624 of climate change on the future of biodiversity. *Ecology Letters*, *15*(4), 365–377.
625 https://doi.org/10.1111/j.1461-0248.2011.01736.x
626 Blach-Overgaard, A., Svenning, J., Dransfield, J., Greve, M., & Balslev, H. (2010).
627 Determinants of palm species distributions across Africa: The relative roles of
628 climate, non-climatic environmental factors, and spatial constraints. *Ecography*,
629 *33*(2), 380–391. https://doi.org/10.1111/j.1600-0587.2010.06273.x
630 Blois, J. L., Zarnetske, P. L., Fitzpatrick, M. C., & Finnegan, S. (2013). Climate Change
631 and the Past, Present, and Future of Biotic Interactions. *Science*, *341*(6145), 499–
632 504. https://doi.org/10.1126/science.1237184
633 Boali, A., Asgari, H. R., Mohammadian Behbahani, A., Salmanmahiny, A., & Naimi, B.
634 (2024). Remotely sensed desertification modeling using ensemble of machine
635 learning algorithms. *Remote Sensing Applications: Society and Environment*, *34*,
636 101149. https://doi.org/10.1016/j.rsase.2024.101149

637 Breiman, L. (2001). Random Forests. *Machine Learning*, *45*, 5–32.
638 https://doi.org/10.1023/A:1010933404324
639 Brun, P., Thuiller, W., Chauvier, Y., Pellissier, L., Wüest, R. O., Wang, Z., &
640 Zimmermann, N. E. (2020). Model complexity affects species distribution
641 projections under climate change. *Journal of Biogeography*, *47*(1), 130–142.
642 https://doi.org/10.1111/jbi.13734
643 Brun, P., Zimmermann, N. E., Hari, C., Pellissier, L., & Karger, D. N. (2022). Global
644 climate-related predictors at kilometer resolution for the past and future. *Earth*
645 *System Science Data*, *14*(12), 5573–5603. https://doi.org/10.5194/essd-14-5573-
646 2022
647 Cardoso Vieira, M., Pischke Garske, R., De Souza Rocha, P., Da Fontoura Xavier Costa,
648 L., Nunes Paiva, A. R., & Thys, R. C. S. (2023). Babassu Mesocarp Flour: A
649 Nutritive Brazilian By-product for Gluten-free Muffins. *Journal of Culinary*
650 *Science & Technology*, *21*(4), 517–532.
651 https://doi.org/10.1080/15428052.2021.1971132
652 Cavallari, M. M., & Toledo, M. M. (2016). What is the name of the babassu? A note on
653 the confusing use of scientific names for this important palm tree. *Rodriguésia*,
654 *67*(2), 533–538. https://doi.org/10.1590/2175-7860201667218
655 Corrêa, B. A., Pimenta, A. S., De Melo, R. R., De Medeiros Neto, P. N., & De Azevedo,
656 T. K. B. (2023). Changes in Land Use and Occupation and Their Implications for
657 the Production Chain of Non-forest Timber Products from Babassu (Attalea
658 speciosa) in the Cocais Region, Maranhão State, Brazil. Em E. C. De Souza & S.
659 S. Muthu (Orgs.), *Forest Science* (p. 167–182). Springer Nature Singapore.
660 https://doi.org/10.1007/978-981-99-2846-0_8

661 Costa, M. F., Francisconi, A. F., Vancine, M. H., & Zucchi, M. I. (2022). Climate change
662 impacts on the *Copernicia alba* and *Copernicia prunifera* (Arecaceae)
663 distribution in South America. *Brazilian Journal of Botany*, *45*(2), 807–818.
664 https://doi.org/10.1007/s40415-022-00801-8
665 De Kort, H., Prunier, J. G., Ducatez, S., Honnay, O., Baguette, M., Stevens, V. M., &
666 Blanchet, S. (2021). Life history, climate and biogeography interactively affect
667 worldwide genetic diversity of plant and animal populations. *Nature*
668 *Communications*, *12*(1), 516. https://doi.org/10.1038/s41467-021-20958-2
669 De Lima, T. M., Portela, R. D. C. Q., Mendes, E. T. B., & Oda, G. A. (2022). Species
670 distribution modeling allied with land-use reveal priority sites and species for
671 palm (Arecaceae) conservation in Rio de Janeiro, Brazil. *Frontiers in Forests and*
672 *Global Change*, *5*, 928446. https://doi.org/10.3389/ffgc.2022.928446
673 De Oliveira, J. A. P., Mukhi, U., Quental, C., & De Oliveira Cerqueira Fortes, P. J. (2022).
674 Connecting businesses and biodiversity conservation through community
675 organizing: The case of babassu breaker women in Brazil. *Business Strategy and*
676 *the Environment*, *31*(5), 2618–2634. https://doi.org/10.1002/bse.3134
677 Dormann, C. F., Elith, J., Bacher, S., Buchmann, C., Carl, G., Carré, G., Marquéz, J. R.
678 G., Gruber, B., Lafourcade, B., Leitão, P. J., Münkemüller, T., McClean, C.,
679 Osborne, P. E., Reineking, B., Schröder, B., Skidmore, A. K., Zurell, D., &
680 Lautenbach, S. (2013). Collinearity: A review of methods to deal with it and a
681 simulation study evaluating their performance. *Ecography*, *36*(1), 27–46.
682 https://doi.org/10.1111/j.1600-0587.2012.07348.x
683 Eiserhardt, W. L., Svenning, J.-C., Kissling, W. D., & Balslev, H. (2011). Geographical
684 ecology of the palms (Arecaceae): Determinants of diversity and distributions

across spatial scales. *Annals of Botany*, *108*(8), 1391–1416. https://doi.org/10.1093/aob/mcr146

Elith, J., & Franklin, J. (2013). Species Distribution Modeling. Em *Encyclopedia of Biodiversity* (p. 692–705). Elsevier. https://doi.org/10.1016/B978-0-12-384719-5.00318-X

Elliott, C. P., Tomlinson, S., Lewandrowski, W., & Miller, B. P. (2024). Species distribution and habitat attributes guide translocation planning of a threatened short-range endemic plant. *Global Ecology and Conservation*, *51*, e02915. https://doi.org/10.1016/j.gecco.2024.e02915

Franklin, J. (2010). *Mapping Species Distributions: Spatial Inference and Prediction* (1º ed). Cambridge University Press. https://doi.org/10.1017/CBO9780511810602

Franklin, J. (2023). Species distribution modelling supports the study of past, present and future biogeographies. *Journal of Biogeography*, *50*(9), 1533–1545. https://doi.org/10.1111/jbi.14617

Frans, V. F., Augé, A. A., Fyfe, J., Zhang, Y., McNally, N., Edelhoff, H., Balkenhol, N., & Engler, J. O. (2022). Integrated SDM database: Enhancing the relevance and utility of species distribution models in conservation management. *Methods in Ecology and Evolution*, *13*(1), 243–261. https://doi.org/10.1111/2041-210X.13736

Freer, J. J., Partridge, J. C., Tarling, G. A., Collins, M. A., & Genner, M. J. (2018). Predicting ecological responses in a changing ocean: The effects of future climate uncertainty. *Marine Biology*, *165*(1), 7. https://doi.org/10.1007/s00227-017-3239-1

Freitas, C., Meerow, A. W., Pintaud, J.-C., Henderson, A., Noblick, L., Costa, F. R. C., Barbosa, C. E., & Barrington, D. (2016). Phylogenetic analysis of *Attalea*

(Arecaceae): Insights into the historical biogeography of a recently diversified Neotropical plant group. *Botanical Journal of the Linnean Society*, *182*(2), 287–302. https://doi.org/10.1111/boj.12466

Friedman, J. H. (2001). Greedy function approximation: A gradient boosting machine. *The Annals of Statistics*, *29*(5). https://doi.org/10.1214/aos/1013203451

Gehring, C., Zelarayán, Ma. C., Luz, R. L., Almeida, R. B., Boddey, R. M., & Leite, M. F. A. (2020). Babassu palm (*Attalea speciosa* Mart.) super-dominance shapes its surroundings via multiple biotic, soil chemical, and physical interactions and accumulates soil carbon: A case study in eastern Amazonia. *Plant Soil*, *454*, 447–460. https://doi.org/10.1007/s11104-020-04580-7

Graham, M. H. (2003). CONFRONTING MULTICOLLINEARITY IN ECOLOGICAL MULTIPLE REGRESSION. *Ecology*, *84*(11), 2809–2815. https://doi.org/10.1890/02-3114

Guisan, A., & Thuiller, W. (2005). Predicting species distribution: Offering more than simple habitat models. *Ecology Letters*, *8*(9), 993–1009. https://doi.org/10.1111/j.1461-0248.2005.00792.x

Guisan, A., & Zimmermann, N. E. (2000). Predictive habitat distribution models in ecology. *Ecological Modelling*, *135*(2–3), 147–186. https://doi.org/10.1016/S0304-3800(00)00354-9

Hao, T., Elith, J., Guillera-Arroita, G., & Lahoz-Monfort, J. J. (2019). A review of evidence about use and performance of species distribution modelling ensembles like BIOMOD. *Diversity and Distributions*, *25*(5), 839–852. https://doi.org/10.1111/ddi.12892

733 Hausfather, Z., & Peters, G. P. (2020). Emissions – the 'business as usual' story is
734 misleading. *Nature*, *577*(7792), 618–620. https://doi.org/10.1038/d41586-020-
735 00177-3
736 Hijman, R., Phillips, S., Leathwick, J., & Elith, J. (2024). *dismo: Species Distribution*
737 *Modeling*. https://github.com/rspatial/dismo
738 Jiménez-Valverde, A. (2014). Threshold-dependence as a desirable attribute for
739 discrimination assessment: Implications for the evaluation of species distribution
740 models. *Biodiversity and Conservation*, *23*(2), 369–385.
741 https://doi.org/10.1007/s10531-013-0606-1
742 Kaky, E., Nolan, V., Alatawi, A., & Gilbert, F. (2020). A comparison between Ensemble
743 and MaxEnt species distribution modelling approaches for conservation: A case
744 study with Egyptian medicinal plants. *Ecological Informatics*, *60*, 101150.
745 https://doi.org/10.1016/j.ecoinf.2020.101150
746 Karger, D. N., Conrad, O., Böhner, J., Kawohl, T., Kreft, H., Soria-Auza, R. W.,
747 Zimmermann, N. E., Linder, H. P., & Kessler, M. (2017). Climatologies at high
748 resolution for the earth's land surface areas. *Scientific Data*, *4*(1), 170122.
749 https://doi.org/10.1038/sdata.2017.122
750 Karger, D. N., Schmatz, D. R., Dettling, G., & Zimmermann, N. E. (2020). High-
751 resolution monthly precipitation and temperature time series from 2006 to 2100.
752 *Scientific Data*, *7*(1), 248. https://doi.org/10.1038/s41597-020-00587-y
753 Karger, D. N., Wilson, A. M., Mahony, C., Zimmermann, N. E., & Jetz, W. (2021). Global
754 daily 1 km land surface precipitation based on cloud cover-informed downscaling.
755 *Scientific Data*, *8*(1), 307. https://doi.org/10.1038/s41597-021-01084-6
756 Katuwal, H. B., Sharma, H. P., Rokka, P., Bhusal, K. P., Bhattarai, B. P., Koirala, S.,
757 Luitel, S. C., Yadav, S., Sah, G., Baral, H. S., Poudyal, L. P., Wang, L., & Quan,

R.-C. (2023). The effects of climate and land use change on the potential distribution and nesting habitat of the Lesser Adjutant in Nepal. *Avian Research*, *14*, 100105. https://doi.org/10.1016/j.avrs.2023.100105

Kissling, W. D., Baker, W. J., Balslev, H., Barfod, A. S., Borchsenius, F., Dransfield, J., Govaerts, R., & Svenning, J. (2012). Quaternary and pre-Quaternary historical legacies in the global distribution of a major tropical plant lineage. *Global Ecology and Biogeography*, *21*(9), 909–921. https://doi.org/10.1111/j.1466-8238.2011.00728.x

Lake, T. A., Briscoe Runquist, R. D., & Moeller, D. A. (2020). Predicting range expansion of invasive species: Pitfalls and best practices for obtaining biologically realistic projections. *Diversity and Distributions*, *26*(12), 1767–1779. https://doi.org/10.1111/ddi.13161

Lannuzel, G., Balmot, J., Dubos, N., Thibault, M., & Fogliani, B. (2021). High-resolution topographic variables accurately predict the distribution of rare plant species for conservation area selection in a narrow-endemism hotspot in New Caledonia. *Biodiversity and Conservation*, *30*(4), 963–990. https://doi.org/10.1007/s10531-021-02126-6

Lee, W.-H., Song, J.-W., Yoon, S.-H., & Jung, J.-M. (2022). Spatial Evaluation of Machine Learning-Based Species Distribution Models for Prediction of Invasive Ant Species Distribution. *Applied Sciences*, *12*(20), 10260. https://doi.org/10.3390/app122010260

Lee-Yaw, J. A., L. McCune, J., Pironon, S., & N. Sheth, S. (2022). Species distribution models rarely predict the biology of real populations. *Ecography*, *2022*(6), e05877. https://doi.org/10.1111/ecog.05877

782 Lima, E. S., Felfili, J. M., Marimon, B. S., & Scariot, A. (2003). Diversidade, estrutura e
783 distribuição espacial de palmeiras em um cerrado sensu stricto no Brasil Central—
784 DF. *Revista Brasileira de Botânica*, *26*(3), 361–370.
785 https://doi.org/10.1590/S0100-84042003000300009
786 Liu, C., Newell, G., & White, M. (2016). On the selection of thresholds for predicting
787 species occurrence with presence-only data. *Ecology and Evolution*, *6*(1), 337–
788 348. https://doi.org/10.1002/ece3.1878
789 Liu, C., White, M., & Newell, G. (2013). Selecting thresholds for the prediction of species
790 occurrence with presence-only data. *Journal of Biogeography*, *40*(4), 778–789.
791 https://doi.org/10.1111/jbi.12058
792 Maltby, K. M., Rutterford, L. A., Tinker, J., Genner, M. J., & Simpson, S. D. (2020).
793 Projected impacts of warming seas on commercially fished species at a
794 biogeographic boundary of the European continental shelf. *Journal of Applied*
795 *Ecology*, *57*(11), 2222–2233. https://doi.org/10.1111/1365-2664.13724
796 Marmion, M., Parviainen, M., Luoto, M., Heikkinen, R. K., & Thuiller, W. (2009).
797 Evaluation of consensus methods in predictive species distribution modelling.
798 *Diversity and Distributions*, *15*(1), 59–69. https://doi.org/10.1111/j.1472-
799 4642.2008.00491.x
800 Mata, L. R., Moreira, A. L. C., Pinedo, A. S., Gomes, S. M., & Azevedo, V. C. R. (2022).
801 Leaf anatomy as an aid to the taxonomy of the 'babassu' complex (Attalea
802 species). *Flora*, *293*, 152092. https://doi.org/10.1016/j.flora.2022.152092
803 McCullagh, P., & Nelder, J. A. (1989). *Generalized Linear Models* (1º ed).
804 Menezes, I. S., Rocha, D. S. B., Voeks, R., Lima Do Couto-Santos, A. P., & Funch, L. S.
805 (2023). Conservation challenges to the useful neotropical palm Babaçu (*Attalea*

pindobassu Bondar) in the face of climate change. *Flora*, *302*, 152262. https://doi.org/10.1016/j.flora.2023.152262

Mitja, D., Sirakov, N., Moreira Dos Santos, A., González-Pérez, S., Jorge Macedo, D., Delaître, E., Demagistri, L., Loisel, P., De Souza Miranda, I., Rey-Valette, H., Da Rocha, M. R. T., Fontez, B., & Libourel, T. (2019). Viability of the Babassu Palm Eco-socio-system in Brazil: The Challenges of Coviability. Em O. Barrière, M. Behnassi, G. David, V. Douzal, M. Fargette, T. Libourel, M. Loireau, L. Pascal, C. Prost, V. Ravena-Cañete, F. Seyler, & S. Morand (Orgs.), *Coviability of Social and Ecological Systems: Reconnecting Mankind to the Biosphere in an Era of Global Change* (p. 257–284). Springer International Publishing. https://doi.org/10.1007/978-3-319-78111-2_14

Naimi, B., & Araújo, M. B. (2016). sdm: A reproducible and extensible R platform for species distribution modelling. *Ecography*, *39*(4), 368–375. https://doi.org/10.1111/ecog.01881

Naimi, B., Hamm, N. A. S., Groen, T. A., Skidmore, A. K., & Toxopeus, A. G. (2014). Where is positional uncertainty a problem for species distribution modelling? *Ecography*, *37*(2), 191–203. https://doi.org/10.1111/j.1600-0587.2013.00205.x

Neto, J. F. D. S., Silva Machado, J., Mendes, F., Rios, M. A. D. S., Assunção, J. C. D. C., Maia Da Silva, F. F., Mathias Macêdo, A. A., & Volken De Souza, C. F. (2021). Aceite de coco babasú (Orbignya speciosa Mart.) extraído industrialmente y manualmente como materia prima para la producción de biodiésel. *Revista ION*, *34*(2). https://doi.org/10.18273/revion.v34n2-2021009

Norberg, A., Abrego, N., Blanchet, F. G., Adler, F. R., Anderson, B. J., Anttila, J., Araújo, M. B., Dallas, T., Dunson, D., Elith, J., Foster, S. D., Fox, R., Franklin, J., Godsoe, W., Guisan, A., O'Hara, B., Hill, N. A., Holt, R. D., Hui, F. K. C., … Ovaskainen,

O. (2019). A comprehensive evaluation of predictive performance of 33 species distribution models at species and community levels. *Ecological Monographs*, *89*(3), e01370. https://doi.org/10.1002/ecm.1370

Nuñez-Penichet, C., Maita, J., & Soberon, J. (2024). Land-cover change in Cuba and implications for the area of distribution of a specialist's host-plant. *PeerJ*, *12*, e17563. https://doi.org/10.7717/peerj.17563

Peterson, A. T., Soberón, J., Pearson, R. G., Anderson, R. P., Martínez-Meyer, E., Nakamura, M., & Araújo, M. B. (2011). *Ecological Niches and Geographic Distributions*. Princeton University Press. https://doi.org/10.1515/9781400840670

Phillips, S. J., Anderson, R. P., & Schapire, R. E. (2006). Maximum entropy modeling of species geographic distributions. *Ecological Modelling*, *190*(3–4), 231–259. https://doi.org/10.1016/j.ecolmodel.2005.03.026

Pintaud, J.-C. (2008). An overview of the taxonomy of Attalea (Arecaceae). *Revista Peruana de Biología*, *15*(3), 055–063. https://doi.org/10.15381/rpb.v15i3.2968

Porro, N., Veiga, I., & Mota, D. (2011). Traditional communities in the Brazilian Amazon and the emergence of new political identities: The struggle of the *quebradeiras de coco babaçu* —babassu breaker women. *Journal of Cultural Geography*, *28*(1), 123–146. https://doi.org/10.1080/08873631.2011.548487

Porro, R. (2019). A economia invisível do babaçu e sua importância para meios de vida em comunidades agroextrativistas. *Bol. Mus. Para. Emílio Goeldi*, *14*(1), 169–188.

Portela, Y. N., Bandeira, D. M., Ferreira, D. D. J., Parente, H. N., Parente, M. D. O. M., Cunha, I. A. L. D., Gois, G. C., Campos, F. S., Sousa, F. C. D. S. D., Rodrigues, L. M. P., Oliveira, J. M. D. S., & Zanine, A. D. M. (2024). By-Products of the

Babassu Agribusiness for Ruminant Diets. *Scientifica*, *2024*(1), 5363940. https://doi.org/10.1155/2024/5363940

Qiao, H., Feng, X., Escobar, L. E., Peterson, A. T., Soberón, J., Zhu, G., & Papeş, M. (2019). An evaluation of transferability of ecological niche models. *Ecography*, *42*(3), 521–534. https://doi.org/10.1111/ecog.03986

Radomski, T., Beamer, D., Babineau, A., Wilson, C., Pechmann, J., & Kozak, K. H. (2022). Finding what you don't know: Testing SDM methods for poorly known species. *Diversity and Distributions*, *28*(9), 1769–1780. https://doi.org/10.1111/ddi.13536

Reis, V. R. R., Deon, D. S., Muniz, L. C., Garcia, U. S., Cantanhêde, I. S. D. L., Moraes Rego, C. A. R. D., Costa, J. B., & Marques, E. D. O. (2018). Soil Chemical Attributes under Crop-Livestock-Forest Integration System and in Different Land Uses in Mata dos Cocais Region. *Journal of Agricultural Science*, *10*(4), 370. https://doi.org/10.5539/jas.v10n4p370

Renner, I. W., Elith, J., Baddeley, A., Fithian, W., Hastie, T., Phillips, S. J., Popovic, G., & Warton, D. I. (2015). Point process models for presence-only analysis. *Methods in Ecology and Evolution*, *6*(4), 366–379. https://doi.org/10.1111/2041-210X.12352

Ressiore, A. C., Lima, C. L. S., & Turnhout, E. (2024). Care narratives: Babassu breakers and mother palm trees. *Geoforum*, *156*, 104109. https://doi.org/10.1016/j.geoforum.2024.104109

Riahi, K., Van Vuuren, D. P., Kriegler, E., Edmonds, J., O'Neill, B. C., Fujimori, S., Bauer, N., Calvin, K., Dellink, R., Fricko, O., Lutz, W., Popp, A., Cuaresma, J. C., Kc, S., Leimbach, M., Jiang, L., Kram, T., Rao, S., Emmerling, J., … Tavoni, M. (2017). The Shared Socioeconomic Pathways and their energy, land use, and

greenhouse gas emissions implications: An overview. *Global Environmental Change*, *42*, 153–168. https://doi.org/10.1016/j.gloenvcha.2016.05.009

Rosenblatt, A. E., & Schmitz, O. J. (2014). Interactive effects of multiple climate change variables on trophic interactions: A meta-analysis. *Climate Change Responses*, *1*(1), 8. https://doi.org/10.1186/s40665-014-0008-y

Santos, A. M. D., Mitja, D., Miranda, I. D. S., Loisel, P., Delaître, E., & Demagistri, L. (2022). What is the influence of anthropogenic impact on the population structure of *Attalea speciosa* Mart. Ex Spreng. In the Brazilian Amazonian region? *Acta Botanica Brasilica*, *36*, e2020abb0543. https://doi.org/10.1590/0102-33062020abb0543

Santos-Filho, F. S., Almeida Júnior, E. B., & Soares, C. J. R. S. (2013). COCAIS: ZONA ECOTONAL NATURAL OU ARTIFICIAL? *REVISTA EQUADOR*, *2*(1), 02–13. https://doi.org/10.26694/equador.v2i1.1043

Scafetta, N. (2023). CMIP6 GCM Validation Based on ECS and TCR Ranking for 21st Century Temperature Projections and Risk Assessment. *Atmosphere*, *14*(2), 345. https://doi.org/10.3390/atmos14020345

Shabani, F., Kumar, L., & Ahmadi, M. (2016). A comparison of absolute performance of different correlative and mechanistic species distribution models in an independent area. *Ecology and Evolution*, *6*(16), 5973–5986. https://doi.org/10.1002/ece3.2332

Shiraishi Neto, J. (2017). QUEBRADEIRAS DE COCO: “Babaçu livre” e reservas extrativistas. *Veredas do Direito: Direito Ambiental e Desenvolvimento Sustentável*, *14*(28), 147–166. https://doi.org/10.18623/rvd.v14i28.920

Sillero, N. (2011). What does ecological modelling model? A proposed classification of ecological niche models based on their underlying methods. *Ecological Modelling*, *222*(8), 1343–1346. https://doi.org/10.1016/j.ecolmodel.2011.01.018

Silva, G. C., Solís Neffa, V. G., Zuquim, G., & Balslev, H. (2023). Biogeography and environmental preferences of *Butia yatay* (Mart.) Becc. *Ecology and Evolution*, *13*(11), e10749. https://doi.org/10.1002/ece3.10749

Silva, M. C. D., Da Silva, L. M., Brandão, K. S., Souza, A. G., Cardoso, L. P., & Dos Santos, A. O. (2014). Low temperature properties of winterized methyl babassu biodiesel. *Journal of Thermal Analysis and Calorimetry*, *115*(1), 635–640. https://doi.org/10.1007/s10973-013-3263-4

Steen, B., Broennimann, O., Maiorano, L., & Guisan, A. (2024). How sensitive are species distribution models to different background point selection strategies? A test with species at various equilibrium levels. *Ecological Modelling*, *493*, 110754. https://doi.org/10.1016/j.ecolmodel.2024.110754

Swets, J. A. (1988). Measuring the Accuracy of Diagnostic Systems. *Science*, *240*, 1285–1293. https://doi.org/10.1126/science.3287615

Teixeira, M. A. (2008). Babassu—A new approach for an ancient Brazilian biomass. *Biomass and Bioenergy*, *32*(9), 857–864. https://doi.org/10.1016/j.biombioe.2007.12.016

Trautmann, S. (2018). *Climate Change Impacts on Birds Species. Bird Species: How They Arise, Modify and Vanish* (D. T. Tietze, Org.). Springer International Publishing. https://doi.org/10.1007/978-3-319-91689-7

Valavi, R., Guillera-Arroita, G., Lahoz-Monfort, J. J., & Elith, J. (2022). Predictive performance of presence-only species distribution models: A benchmark study

with reproducible code. *Ecological Monographs*, *92*(1), e01486. https://doi.org/10.1002/ecm.1486

Vasquez, V. L., De Lima, A. A., Dos Santos, A. P., & Pinto, M. P. (2021). Influence of spatial extent on habitat suitability models for primate species of Atlantic Forest. *Ecological Informatics*, *61*, 101179. https://doi.org/10.1016/j.ecoinf.2020.101179

Vedel-Sørensen, M., Tovaranonte, J., Bøcher, P. K., Balslev, H., & Barfod, A. S. (2013). Spatial distribution and environmental preferences of 10 economically important forest palms in western South America. *Forest Ecology and Management*, *307*, 284–292. https://doi.org/10.1016/j.foreco.2013.07.005

Vieira, A. P., Santana, S. A. A., Bezerra, C. W. B., Silva, H. A. S., Chaves, J. A. P., Melo, J. C. P. D., Silva Filho, E. C. D., & Airoldi, C. (2011). Epicarp and mesocarp of babassu (Orbignya speciosa): Characterization and application in copper phtalocyanine dye removal. *Journal of the Brazilian Chemical Society*, *22*(1), 21–29. https://doi.org/10.1590/S0103-50532011000100003

Volis, S., & Tojibaev, K. (2021). Defining critical habitat for plant species with poor occurrence knowledge and identification of critical habitat networks. *Biodiversity and Conservation*, *30*(12), 3603–3611. https://doi.org/10.1007/s10531-021-02265-w

Whitford, A. M., Shipley, B. R., & McGuire, J. L. (2024). The influence of the number and distribution of background points in presence-background species distribution models. *Ecological Modelling*, *488*, 110604. https://doi.org/10.1016/j.ecolmodel.2023.110604

Zhang, L., Huettmann, F., Liu, S., Sun, P., Yu, Z., Zhang, X., & Mi, C. (2019). Classification and regression with random forests as a standard method for presence-only data SDMs: A future conservation example using China tree

species. *Ecological Informatics*, *52*, 46–56. https://doi.org/10.1016/j.ecoinf.2019.05.003

Zuquim, G., Jones, M. M., Ovaskainen, O., Trujillo, W., & Balslev, H. (2023). The legacy of human use in Amazonian palm communities along environmental and accessibility gradients. *Global Ecology and Biogeography*, *32*(6), 881–892. https://doi.org/10.1111/geb.13667

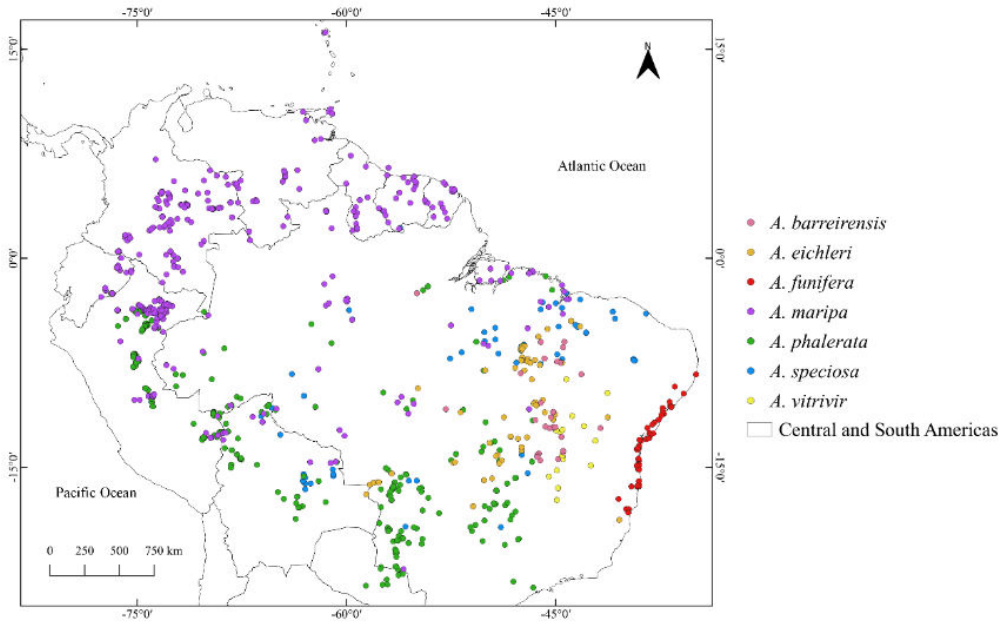

[double column]

Figure 1. Distribution map of occurrence points obtained from the GBIF database for the Babassu Complex species: *A. phalerata* (n = 15,170), *A. maripa* (n = 3,580), *A. eichleri* (n = 142), *A. speciosa* (n = 129), *A. funifera* (n = 84), *A. barreirensis* (n = 52), and *A. vitrivir* (n = 47).

967 a)

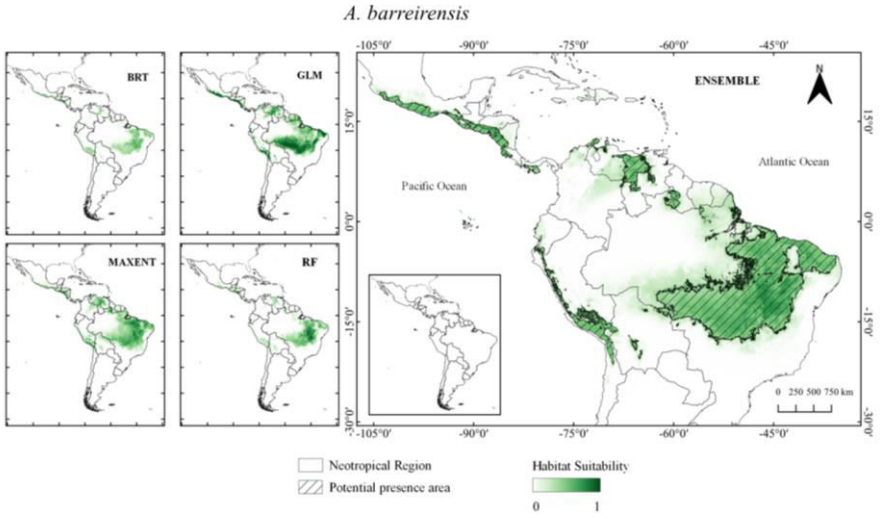

968

969 b)

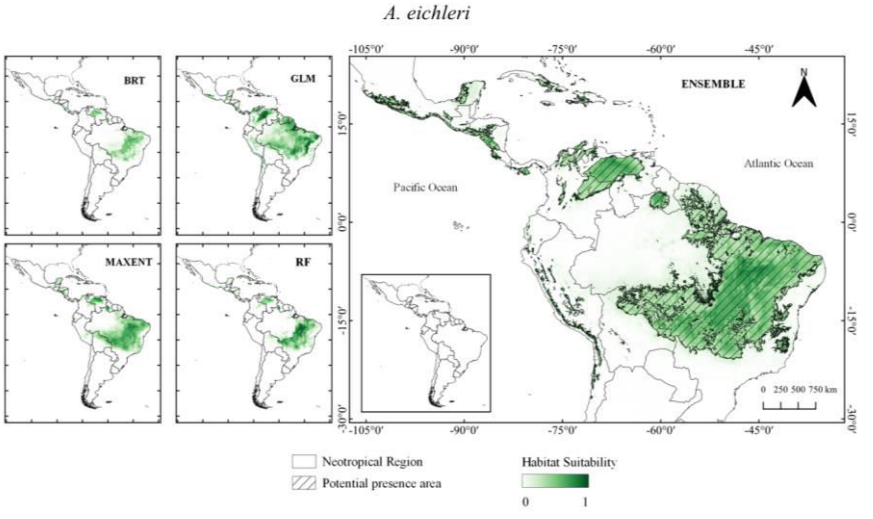

970

971 c)

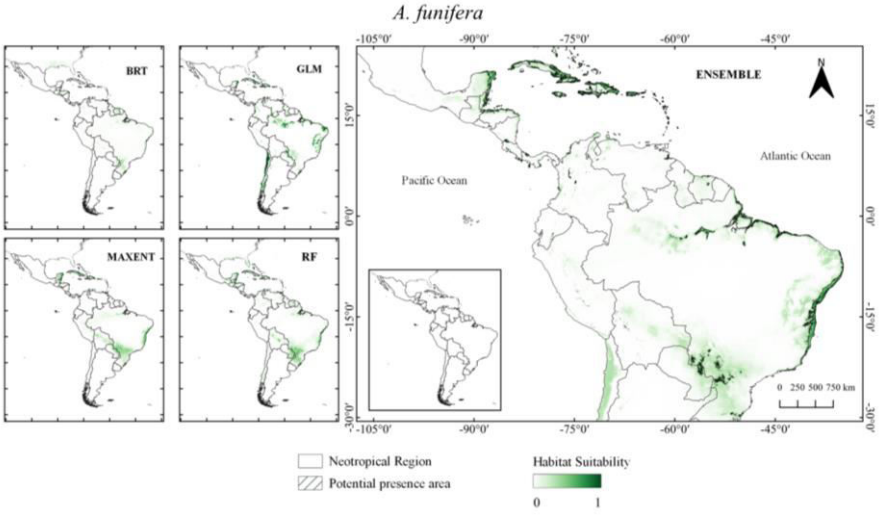

972

973 d)

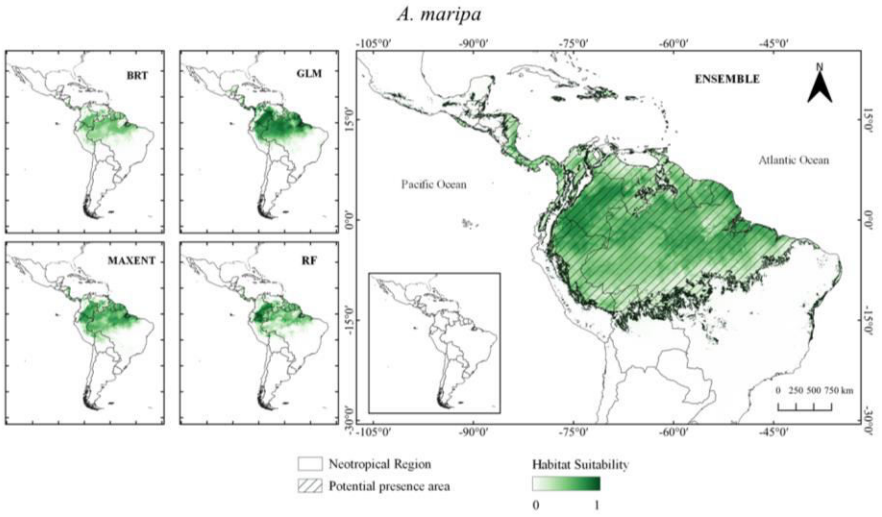

974

975 e)

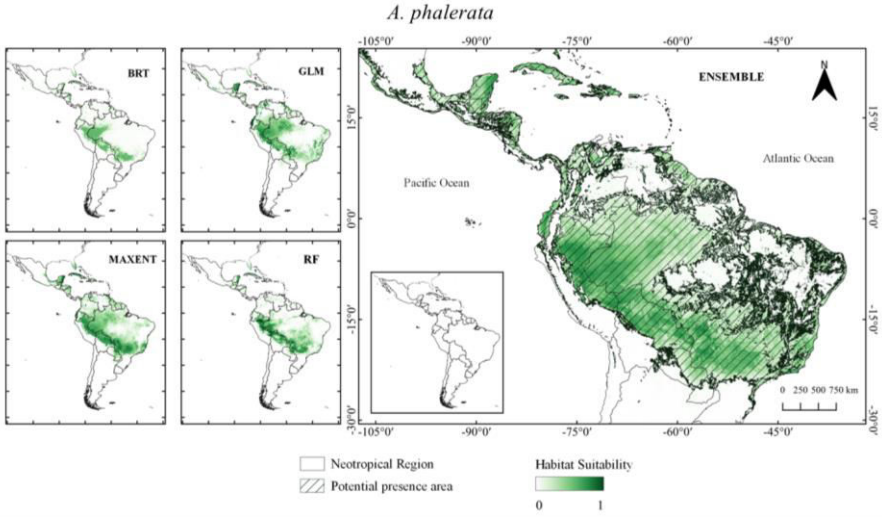

976

977 f)

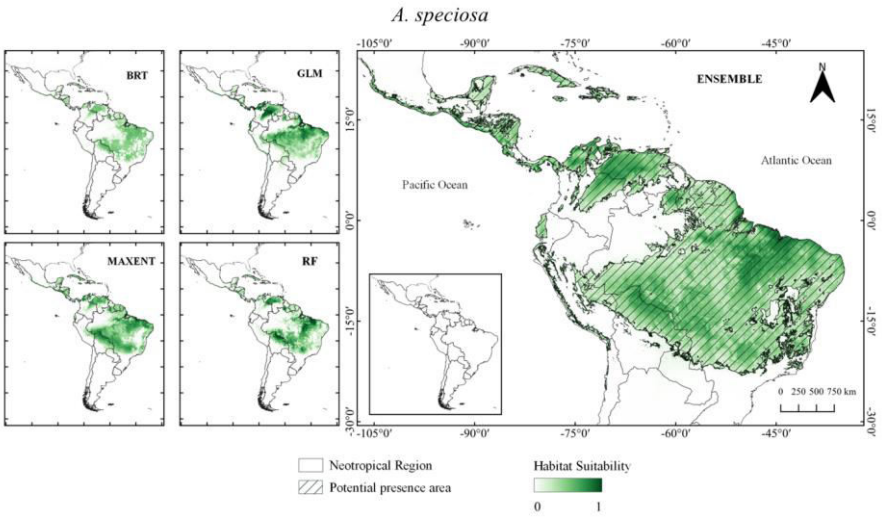

978

979 g)

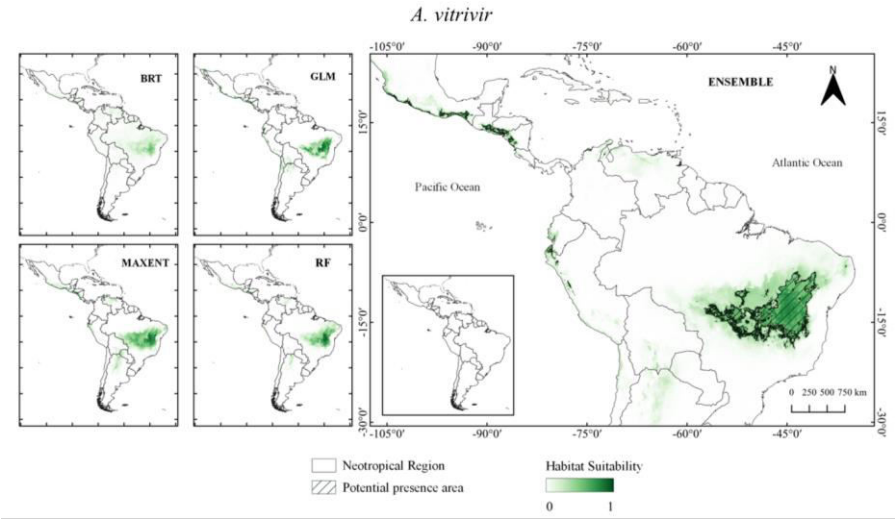

h)

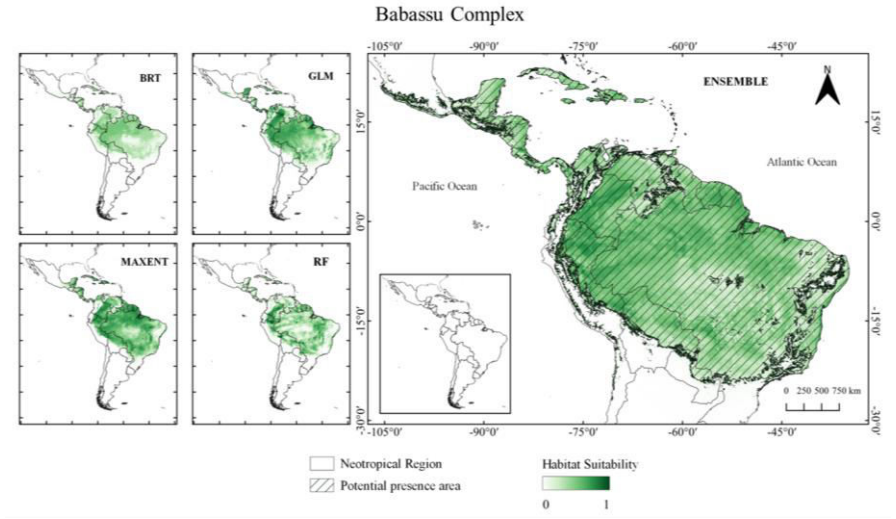

[double column]

Figure 2. Habitat suitability maps for the modelled distribution of species within the Babassu Complex, based on Maximum Entropy (Maxent), Random Forest (RF), Boosted Regression Trees (BRT), Generalized Linear Models (GLM), and the ensemble map of all algorithms. The maps represent: a) *A. barreirensis*, b) *A. eichleri*, c) *A. funifera*, d) *A. maripa*, e) *A. phalerata*, f) *A. speciosa*, g) *A. vitrivir*, and h) the Babassu Complex overall, covering Neotropical region.

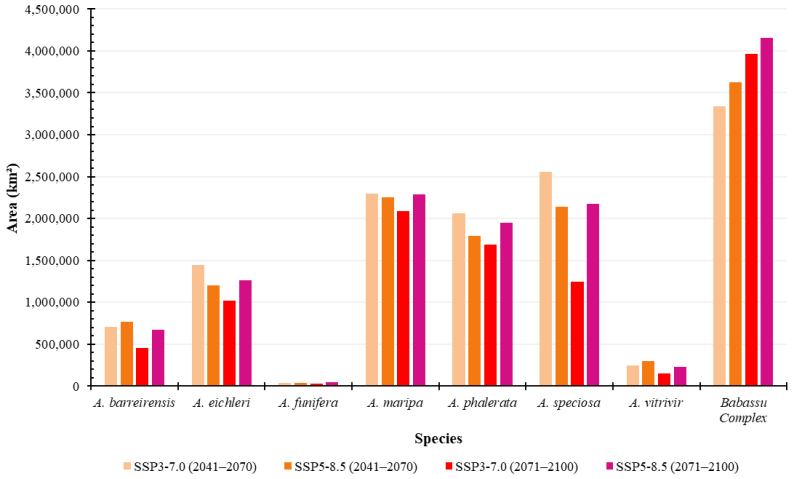

[single column]

Figure 3. Projected area (km²) of high environmental Suitability for seven *Attalea* species and the Babassu Complex under SSP3-7.0 and SSP5-8.5 scenarios for 2041–2070 and 2071–2100.

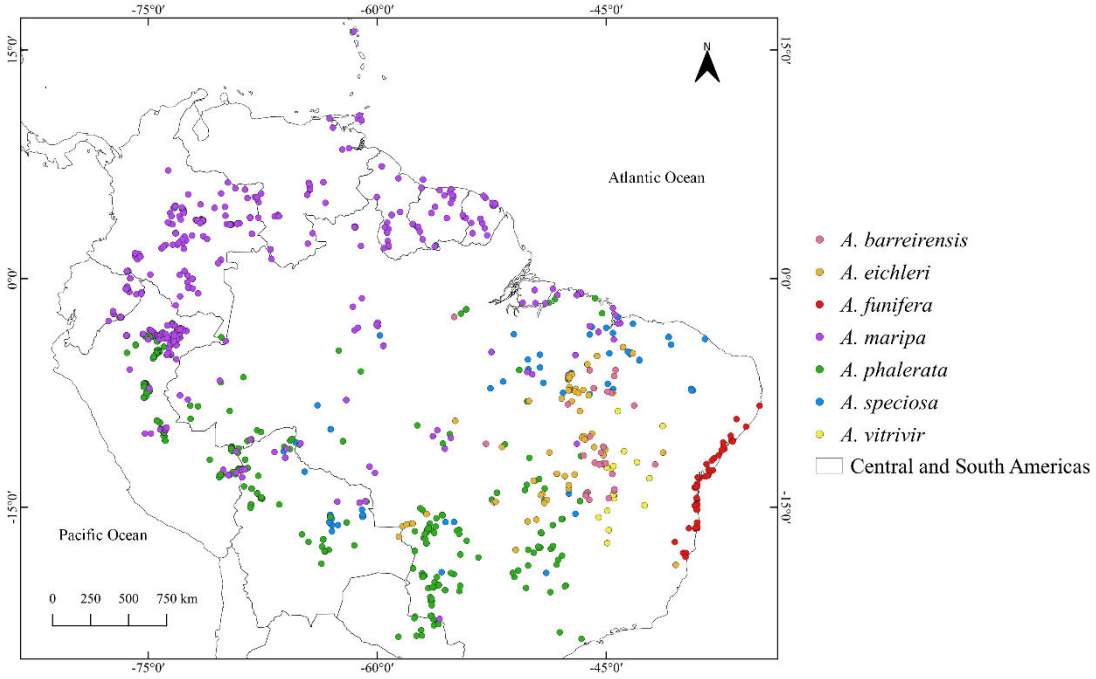

Figure 1. Distribution map of occurrence points obtained from the GBIF database for the Babassu Complex species: *A. phalerata* (n = 15,170), *A. maripa* (n = 3,580), *A. eichleri* (n = 142), *A. speciosa* (n = 129), *A. funifera* (n = 84), *A. barreirensis* (n = 52), and *A. vitrivir* (n = 47).

a)

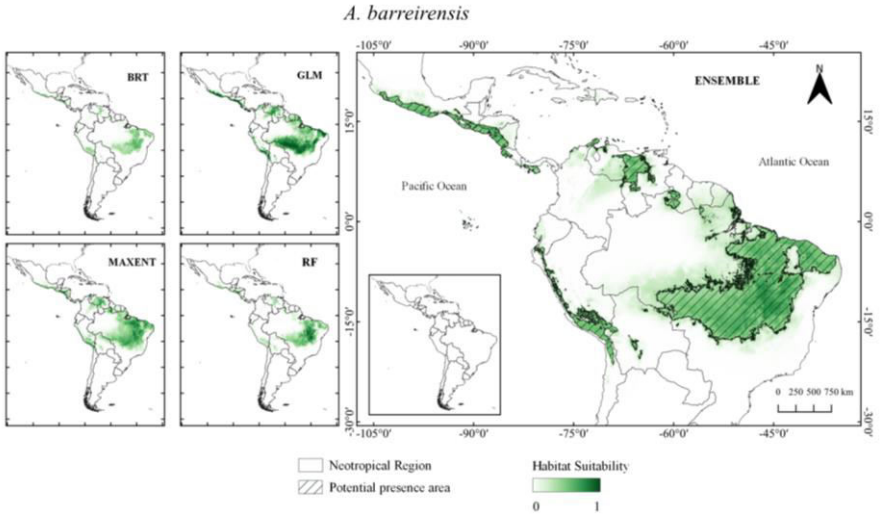
A. barreirensis
BRT
GLM
MAXENT
RF
ENSEMBLE
Pacific Ocean
Atlantic Ocean
-105°0'
-90°0'
-75°0'
-60°0'
-45°0'
15°0'
0°0'
-15°0'
-30°0'
0 250 500 750 km
Neotropical Region
Potential presence area
Habitat Suitability
0
1

b)

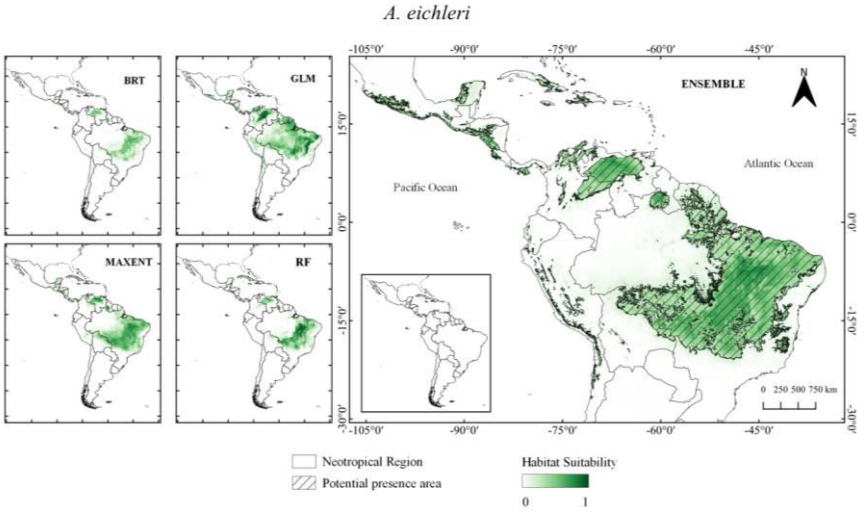
A. eichleri
BRT
GLM
MAXENT
RF
ENSEMBLE
Pacific Ocean
Atlantic Ocean
-105°0'
-90°0'
-75°0'
-60°0'
-45°0'
15°0'
0°0'
-15°0'
-30°0'
0 250 500 750 km
Neotropical Region
Potential presence area
Habitat Suitability
0
1

c)

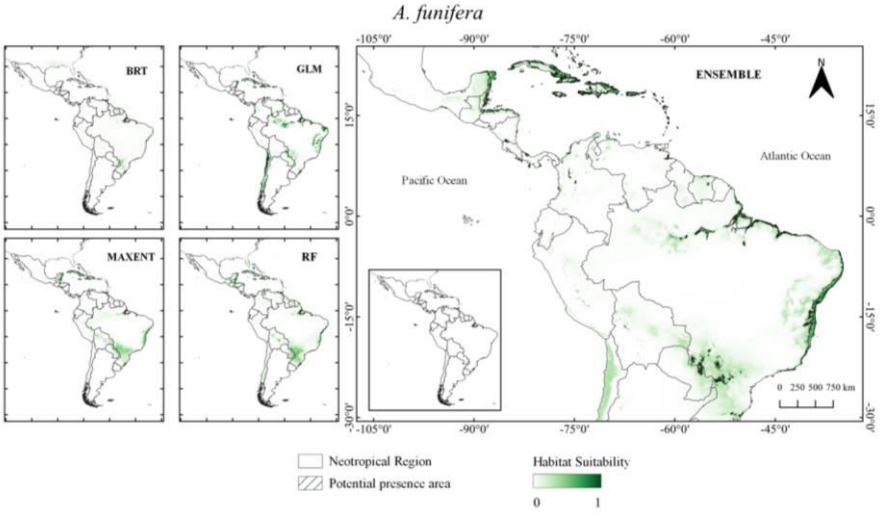
A. funifera
BRT
GLM
MAXENT
RF
ENSEMBLE
Pacific Ocean
Atlantic Ocean
-105°0'
-90°0'
-75°0'
-60°0'
-45°0'
15°0'
0°0'
-15°0'
-30°0'
0 250 500 750 km
Neotropical Region
Potential presence area
Habitat Suitability
0
1

d)

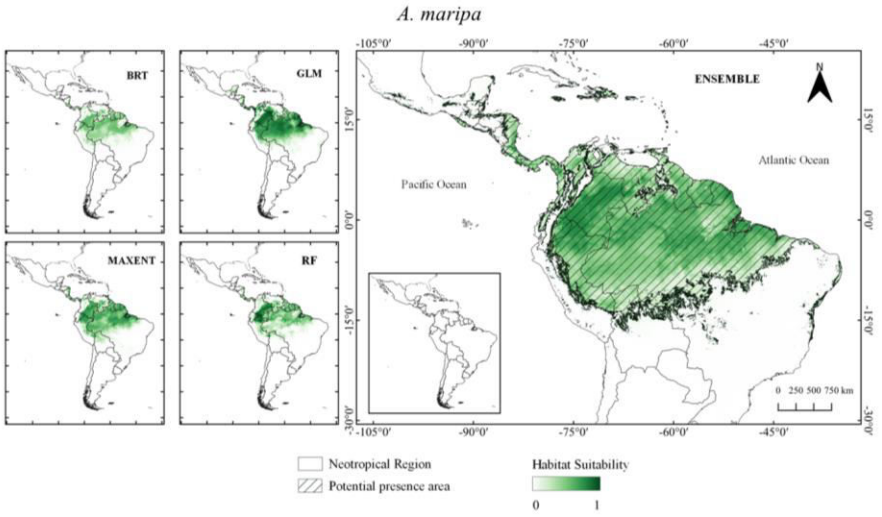
A. maripa
BRT
GLM
MAXENT
RF
ENSEMBLE
Pacific Ocean
Atlantic Ocean
0 250 500 750 km
Neotropical Region
Potential presence area
Habitat Suitability
0
1

e)

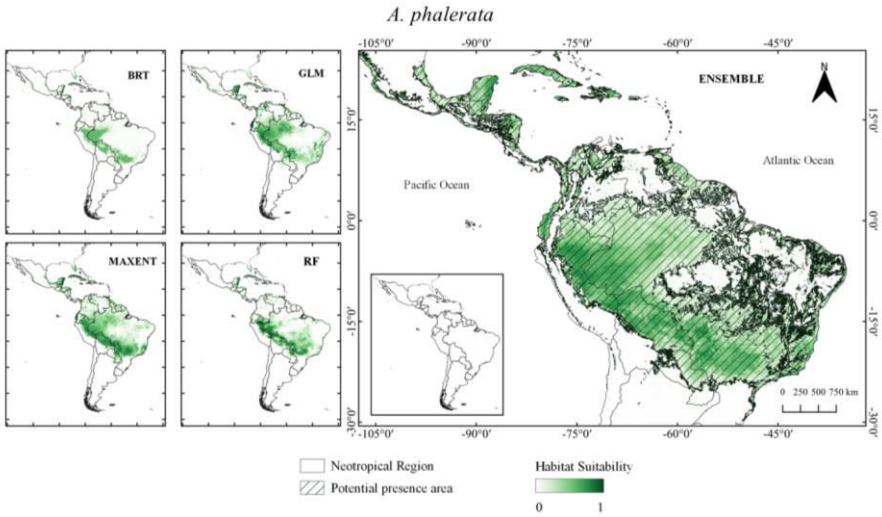
A. phalerata
BRT
GLM
MAXENT
RF
ENSEMBLE
Pacific Ocean
Atlantic Ocean
0 250 500 750 km
Neotropical Region
Potential presence area
Habitat Suitability
0
1

f)

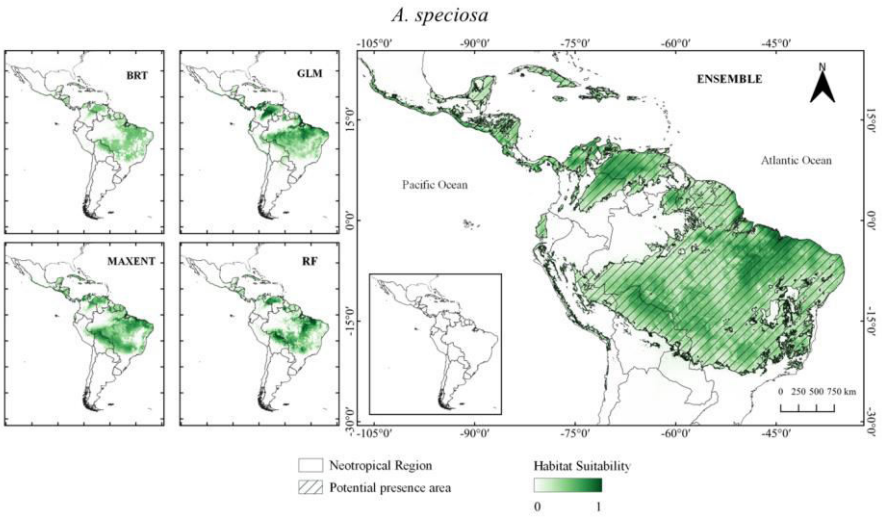
A. speciosa
BRT
GLM
MAXENT
RF
ENSEMBLE
Pacific Ocean
Atlantic Ocean
0 250 500 750 km
Neotropical Region
Potential presence area
Habitat Suitability
0
1

g)

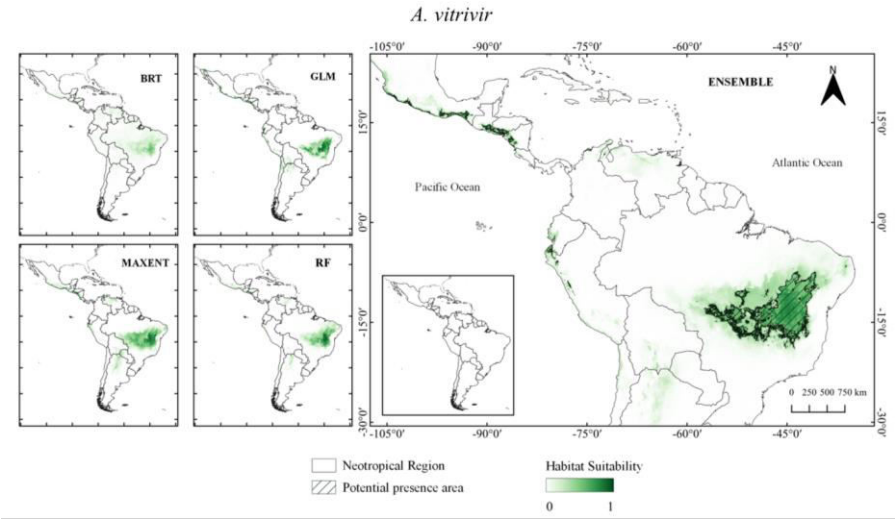

h)

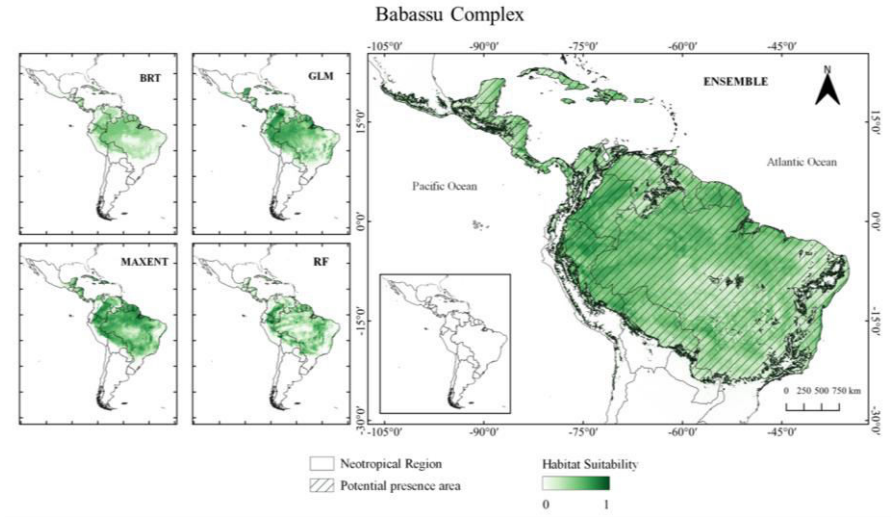

Figure 2. Habitat suitability maps for the modelled distribution of species within the Babassu Complex, based on Maximum Entropy (Maxent), Random Forest (RF), Boosted Regression Trees (BRT), Generalized Linear Models (GLM), and the ensemble map of all algorithms. The maps represent: a) *A. barreirensis*, b) *A. eichleri*, c) *A. funifera*, d) *A. maripa*, e) *A. phalerata*, f) *A. speciosa*, g) *A. vitrivir*, and h) the Babassu Complex overall, covering Neotropical region.

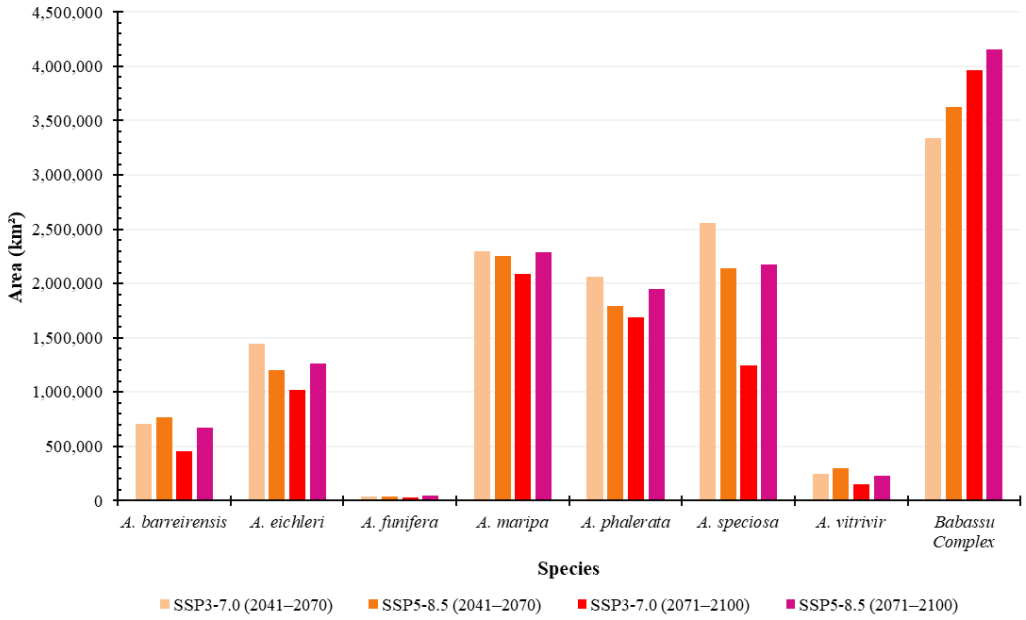

Figure 3. Projected area (km²) of high environmental Suitability for seven *Attalea* species and the Babassu Complex under SSP3-7.0 and SSP5-8.5 scenarios for 2041–2070 and 2071–2100.

Table 1. Projected changes in habitat suitability for *A. barreirensis*, *A. eichleri*, *A. funifera*, *A. maripa*, *A. phalerata*, *A. speciosa*, *A. vitrivir*, and the Babassu Complex overall, under SSP3-7.0 and SSP5-8.5 Scenarios (2041-2100 and 2071-2100).

Species	Class	Scenarios							
		2041-2070				2071-2100			
		SSP3 - 7.0		SSP5 - 8.5		SSP3 - 7.0		SSP5 - 8.5	
		Future (km²)	Relative Difference (%)	Future (km²)	Relative Difference (%)	Future (km²)	Relative Difference (%)	Future (km²)	Relative Difference (%)
A. barreirensis	Unsuitable	10389998	-12.78	11222328	-5.79	10599801	-11.02	9662624	-18.89
	Low	7550859	16.80	7037553	8.86	8265168	27.85	8340284	29.01
	Medium	2922591	-1.32	2547970	-13.97	2255124	-23.86	2898266	-2.14
	High	710311	178.68	765908	200.49	453666	77.99	672586	163.88
A. eichleri	Unsuitable	10203525	0.14	9851437	-3.31	10266276	0.76	9234843	-9.37
	Low	6931939	-17.64	7564985	-10.11	7192470	-14.54	8121934	-3.50
	Medium	2990210	13.09	2956637	11.82	3092123	16.95	2954888	11.76
	High	1448086	319.90	1200700	248.17	1022890	196.61	1262094	265.97
A. funifera	Unsuitable	4114133	-70.66	6004479	-57.17	6964763	-50.32	4544225	-67.59
	Low	16657799	133.94	15181583	113.21	14352789	101.57	16447072	130.98
	Medium	764255	81.03	351878	-16.65	227706	-46.06	535694	26.89
	High	37572	20.56	35819	14.93	28501	-8.55	46769	50.06
A. maripa	Unsuitable	9145010	-22.61	9146797	-22.60	8997537	-23.86	8997711	-23.86
	Low	5799128	25.04	5650332	21.83	5878972	26.76	5713825	23.20

	Medium	4334464	2.63	4524891	7.14	4608890	9.13	4573014	8.28
	High	2295158	150.70	2251740	145.96	2088360	128.11	2289209	150.05
A. phalerata	Unsuitable	5762009	-25.74	6098864	-21.40	5855616	-24.53	6262523	-19.29
	Low	7905634	-20.43	8162661	-17.84	8303156	-16.43	6851348	-31.04
	Medium	5847963	84.71	5519804	74.35	5729364	80.97	6509678	105.61
	High	2058153	180.65	1792430	144.41	1685624	129.85	1950210	165.93
A. speciosa	Unsuitable	6270546	-33.72	7329885	-22.52	7834524	-17.19	7098530	-24.97
	Low	7670282	16.46	7065532	7.28	7171222	8.89	7443843	13.03
	Medium	5073102	9.80	5042139	9.13	5321250	15.17	4859595	5.18
	High	2559830	175.99	2136203	130.32	1246764	34.42	2171792	134.15
A. vitrivir	Unsuitable	12884926	-11.15	12859357	-11.33	13861406	-4.42	13051311	-10.01
	Low	7484122	28.60	6857590	17.84	6962269	19.63	6860189	17.88
	Medium	954730	-12.12	1562079	43.79	603198	-44.47	1435779	32.17
	High	249982	34.50	294734	58.58	146886	-20.97	226480	21.86
Babassu Complex	Unsuitable	6188662	-17.12	6515732	-12.75	6032378	-19.22	6087909	-18.47
	Low	4050732	-30.26	4004980	-31.05	4030283	-30.61	4009590	-30.97
	Medium	7997410	1.35	7431489	-5.83	7547891	-4.35	7322919	-7.20
	High	3336956	680.78	3621558	747.37	3963208	827.31	4153342	871.80

Table S1.1. ODMAP protocol documenting the modelling workflow for climate change projections of seven Attalea species (Babassu Complex) in the Neotropics.

1. Overview	**1.1 Objective**	To identify the key bioclimatic drivers of the Babassu Complex (*Attalea* spp.) in the Neotropics and predict current and future habitat suitability under climate change scenarios.
	1.2 Study Taxa	Babassu Complex (*Attalea* spp.) – Seven species: *A. barreirensis*, *A. eichleri*, *A. funifera*, *A. maripa*, *A. phalerata*, *A. speciosa*, *A. vitrivir*, and Babassu Complex overall.
	1.3 Study Area	Neotropical Region
	1.4 Study Period	Current (2011-2040); Future (2041–2070 and 2071–2100).
	1.5 Hypotheses	Species distributions will shift due to climate change, expanding for climate-tolerant species and shrinking for climate-sensitive ones.
2. Occurrence Data	**2.1 Source**	GBIF.
	2.2 Data Type	Presence-only records.
	2.3 Sample Size	~19,204 raw records; *A. barreirensis* (n = 41), *A. eichleri* (n = 79), *A. funifera* (n = 65), *A. maripa* (n = 570), *A. phalerata* (n = 431), *A. speciosa* (n = 84), *A. vitrivir* (n = 27), and the combined dataset (n = 1,269), after spatial filtering.
	2.4 Filtering Methods	Spatial thinning to 20 km.
3. Environmental Data	**3.1 Variable Source**	CHELSA v2.1 bioclimatic variables; SMI-CMIP6 GCMs for future scenarios.
	3.2 Variables Used	Full list of 23 CHELSA variables (bio1–bio19, PP, VPD derivatives); reduced post-VIF.
	3.3 Resolution	30 arc-seconds (~1 km²).
	3.4 GCMs Used	GFDL-ESM4, UKESM1-0-LL, MPI-ESM1-2-HR, IPSL-CM6A-LR, MRI-ESM2-0.
	3.5 Scenarios	SSP3-7.0 and SSP5-8.5.
4. Pre-processing	**4.1 Collinearity**	VIF threshold < 10; usdm:vifstep() used.
	4.2 Replacement of Missing Predictors	Spearman correlation with current variables to substitute missing PP and VPD values.
	4.3 Spatial Mask	Entire Neotropical realm.
5. Modelling	**5.1 Algorithms Used**	Maximum Entropy (MaxEnt), Random Forest (RF), Boosted Regression Trees (BRT), Generalized Linear Models (GLM).

	5.2 Pseudo-absences	10,000 randomly selected background points per model.
	5.3 Model Calibration	70% training / 30% testing; k-fold cross-validation (5 folds × 5 repeats).
	5.4 Model Evaluation	AUC, TSS, Deviance.
	5.5 Ensemble Modelling	Weighted mean using TSS for current and future projections.
	5.6 Software	R 4.3.2 (packages: sdm, dismo, usdm, Hmisc, etc.); QGIS 3.18.2.
6. Output	**6.1 Suitability Maps**	Continuous (0–1) and classified maps: unsuitable (≤ 0.05), low (0.05–0.33), medium (0.33–0.66), high (> 0.66).
	6.2 Thresholding	maxSSS (maximizes sensitivity + specificity).
	6.3 Presence-Absence Maps	Ensemble presence-absence per species and overall complex.
	6.4 Area Calculation	Suitability maps reprojected to UTM, 1 km resolution. Area computed for all classes.
	6.5 Change Maps	Area change between current and future for each class and species.
	6.6 Variable Importance	Relative variable contribution (Im%) based on mean AUC-weighted values across repetitions.
7. Uncertainty & Validation	**7.1 Sources of Uncertainty**	Algorithmic, GCM, scenario-specific; addressed via ensembling.
	7.2 Model Robustness	High mean AUC (0.97–0.99), high TSS (0.90–0.95).
	7.3 Data Availability	Data and code archived at Zenodo: https://doi.org/10.5281/zenodo.15243376
8. Interpretation	**8.1 Ecological Implications**	Species with wider tolerance may expand, altering community composition and ecosystem function. Potential ecological disruption vs restoration opportunities.
	8.2 Conservation Relevance	Highlights climate-driven biogeographic shifts in socio-economically important species. Supports regional conservation planning in Amazon and Cerrado biomes.
9. Funding	**9.1 Funding**	FAPEMA (IECT-05539/18), CAPES (PDSE - Edital n° 44/2022).

Table S1.2. List of bioclimatic variables considered for constructing the bioclimatic models sourced from the Climatologies at High Resolution for the Earth's Land Surface Areas (CHELSA) database, version 2.1.

Acronym	Code	Description
APA	bio12	Annual Precipitation Amount
ART	bio7	Annual Range of Air Temperature
Iso	bio3	Isothermality
MAAT	bio1	Mean Annual Air Temperature
MDTCQ	bio11	Mean Daily Mean Air Temperatures of the Coldest Quarter
MDTDQ	bio9	Mean Daily Mean Air Temperatures of the Driest Quarter
MDTR	bio2	Mean Diurnal Temperature Range
MDTWaQ	bio10	Mean Daily Mean Air Temperatures of the Warmest Quarter
MDTWeQ	bio8	Mean Daily Mean Air Temperatures of the Wettest Quarter
MMPACQ	bio19	Mean Monthly Precipitation Amount of the Coldest Quarter
MMPADQ	bio17	Mean Monthly Precipitation Amount of the Driest Quarter
MMPAWaQ	bio18	Mean Monthly Precipitation Amount of the Warmest Quarter
MMPAWeQ	bio16	Mean Monthly Precipitation Amount of the Wettest Quarter
PADM	bio14	Precipitation Amount of the Driest Month
PAWM	bio13	Precipitation Amount of the Wettest Month
PPMax	Pet_penman_max	Maximum monthly potential evapotranspiration
PPMean	Pet_penman_mean	Mean monthly potential evapotranspiration
PPMin	Pet_penman_min	Minimum monthly potential evapotranspiration
PPRange	Pet_penman_range	Annual range of monthly potential evapotranspiration
PS	bio15	Precipitation Seasonality
TMaxW	bio5	Mean Daily Maximum Air Temperature of the Warmest Month
TMinC	bio6	Mean Daily Minimum Air Temperature of the Coldest Month
TS	bio4	Temperature Seasonality
VPDMax	VPDMax	Maximum monthly vapor pressure deficit
VPDMean	VPDMean	Mean monthly vapour pressure deficit
VPDMin	VPDMin	Minimum monthly vapour pressure deficit
VPDRange	VPDRange	Annual range of monthly vapour pressure deficit

Table S1.3. Final predictors retained after multicollinearity testing for each babassu species and the overall Babassu Complex, used for the current scenario and adjusted through correlation analysis for future scenarios.

SPECIES															
A. barreirensis		*A. eichleri*		*A. funifera*		*A. maripa*		*A. phalerata*		*A. speciosa*		*A. vitrivir*		Babassu Complex	
Current	**Future**	**Current**	**Future**	**Current**	**Future**	**Current**	**Future**	**Current**	**Future**	**Current**	**Future**	**Current**	**Future**	**Current**	**Future**
Iso	Iso	Iso	Iso	Iso	Iso	Iso	Iso	MDTDQ	MDTDQ	APA	APA	MDTR	MDTR	Iso	Iso
MDTR	MDTR	MDTR	MDTR	MMPACQ	MMPACQ	MDTDQ	MDTDQ	MDTR	MDTR	Iso	Iso	MDTWeQ	MDTWeQ	MDTR	MDTR
MDTWeQ	MDTWeQ	MDTWeQ	MDTWeQ	MMPAWaQ	MMPAWaQ	MDTR	MDTR	MDTWeQ	MDTWeQ	MDTR	MDTR	MMPACQ	MMPACQ	MDTWeQ	MDTWeQ
MMPAWaQ	MMPAWaQ	MMPACQ	MMPACQ	PADM	PADM	MDTWeQ	MDTWeQ	MMPACQ	MMPACQ	MDTWeQ	MDTWeQ	MMPAWaQ	MMPAWaQ	MMPAWaQ	MMPAWaQ
PAWM	PAWM	MMPAWaQ	MMPAWaQ	PAWM	PAWM	MMPACQ	MMPACQ	MMPAWaQ	MMPAWaQ	MMPACQ	MMPACQ	PADM	PADM	PADM	PADM
PPMin	PADM	PAWM	PAWM	PPMax	MAAT	PADM	PADM	PADM	PADM	MMPAWaQ	MMPAWaQ	PAWM	PAWM	PAWM	PAWM
PPRange	MMPAWaQ	PPMean	MMPADQ	PPRange	MDTCQ	PAWM	PAWM	PAWM	PAWM	PADM	PADM	PPMin	MDTDQ	PPMin	MMPADQ
PS	PS	PPRange	PADM	VPDMean	~~MAAT~~	PPMin	PADM	PPMax	ART	PPMax	MMPADQ	PS	PS	PPRange	TS
TS	TS	PS	PS	VPDRange	ART	PPRange	MMPAWaQ	PPMin	MAAT	PPMin	MDTCQ			PS	PS
		TS	TS			PS	PS	VPDMin	TMaxW	PS	PS			TS	TS
		VPDMin	MDTWeQ			TS	TS	VPDRange	MMPADQ	VPDMin	MDTWeQ			VPDMin	MMPADQ
		VPDRange	TMaxW			VPDMin	MDTWaQ			VPDRange	TMaxW			VPDRange	TMaxW

Table S1.4. Performance values based on a) mean area under the curve (AUC), b) True Skill Statistics (TSS), and c) Deviances, for the potential species distribution modeling using Maxent, Random Forest (RF), Boosted Regression Trees (BRT), and Generalized Linear Models (GLM). Results are provided for each babassu species and the Babassu Complex overall. Values in parentheses represent the standard deviation of the mean (n = 25).

a)

Species	**Algorithms (n=25)**			
	MaxEnt	RF	GLM	BRT
A. barreirensis	0.99 (± 0.01)	0.99 (± 0.01)	0.95 (± 0.02)	0.99 (± 0.01)
A. eichleri	0.99 (± 0.01)	0.99 (± 0.01)	0.96 (± 0.01)	0.99 (± 0.01)
A. funifera	1.00 (± 0.00)	1.00 (± 0.00)	0.99 (± 0.01)	0.99 (± 0.01)
A. maripa	0.99 (± 0.00)	0.99 (± 0.00)	0.98 (± 0.00)	0.99 (± 0.00)
A. phalerata	0.99 (± 0.00)	0.99 (± 0.00)	0.97 (± 0.01)	0.98 (± 0.00)
A. speciosa	0.99 (± 0.01)	0.99 (± 0.00)	0.96 (± 0.01)	0.99 (± 0.01)
A. vitrivir	0.99 (± 0.01)	0.99 (± 0.01)	0.96 (± 0.03)	0.97 (± 0.03)
Babassu Complex	0.98 (± 0.00)	0.99 (± 0.00)	0.97 (± 0.00)	0.97 (± 0.00)
mean (n=200)	0.99 (±0.01)	0.99 (±0.01)	0.97 (±0.02)	0.98 (±0.01)

b)

Species	**Algorithms (n=25)**			
	MaxEnt	RF	GLM	BRT
A. barreirensis	0.96 (± 0.04)	0.95 (± 0.04)	0.90 (± 0.05)	0.93 (± 0.05)
A. eichleri	0.96 (± 0.03)	0.95 (± 0.03)	0.89 (± 0.04)	0.94 (± 0.02)
A. funifera	0.99 (± 0.02)	0.99 (± 0.02)	0.96 (± 0.04)	0.96 (± 0.05)
A. maripa	0.94 (± 0.01)	0.94 (± 0.01)	0.92 (± 0.01)	0.92 (± 0.01)
A. phalerata	0.90 (± 0.03)	0.94 (± 0.02)	0.85 (± 0.02)	0.86 (± 0.02)
A. speciosa	0.94 (± 0.04)	0.95 (± 0.03)	0.90 (± 0.03)	0.93 (± 0.03)
A. vitrivir	0.97 (± 0.02)	0.95 (± 0.06)	0.90 (± 0.05)	0.86 (± 0.06)
Babassu Complex	0.91 (± 0.01)	0.92 (± 0.01)	0.87 (± 0.01)	0.86 (± 0.02)
mean (n=200)	0.94 (±0.04)	0.95 (±0.04)	0.90 (±0.05)	0.91 (±0.05)

c)

Species	**Algorithms (n=25)**			
	MaxEnt	RF	GLM	BRT
A. barreirensis	0.20 (± 0.06)	0.15 (± 0.05)	0.35 (± 0.12)	0.27 (± 0.04)
A. eichleri	0.18 (± 0.05)	0.16 (± 0.04)	0.30 (± 0.05)	0.26 (± 0.02)
A. funifera	0.10 (± 0.02)	0.08 (± 0.02)	0.15 (± 0.09)	0.22 (± 0.04)
A. maripa	0.16 (± 0.01)	0.11 (± 0.01)	0.19 (± 0.02)	0.26 (± 0.01)
A. phalerata	0.19 (± 0.02)	0.12 (± 0.01)	0.25 (± 0.02)	0.29 (± 0.02)
A. speciosa	0.18 (± 0.03)	0.15 (± 0.02)	0.28 (± 0.04)	0.25 (± 0.03)
A. vitrivir	0.21 (± 0.04)	0.17 (± 0.05)	0.37 (± 0.17)	0.32 (± 0.07)
Babassu Complex	0.21 (± 0.01)	0.14 (± 0.01)	0.26 (± 0.01)	0.32 (± 0.01)
mean (n=200)	0.18 (±0.05)	0.13 (±0.04)	0.27 (±0.11)	0.28 (±0.05)

Table 1.5. Relative importance of predictor variables (Im%) per species vs. algorithm combination (n = 25) in explaining the distribution of a) *A. barreirensis*, b) *A. eichleri*, c) *A. funifera*, d) *A. maripa*, e) *A. phalerata*, f) *A. speciosa*, g) *A. vitrivir*, and h) the Babassu Complex overall. The algorithms considered include Maxent, Random Forest (RF), Boosted Regression Trees (BRT), and Generalized Linear Models (GLM). Mean and Coefficient of Variation (CV) values are provided for each bioclimatic predictor (n = 100). Values in parentheses represent the standard deviation of the mean.

a)

Predictors	Algorithms (n=25)				mean (n=100)	CV
	MaxEnt	RF	GLM	BRT		
Iso	1.05 (±1.43)	1.84 (±2.49)	7.80 (±3.24)	2.07 (±1.81)	3.19 (±3.56)	1.11
MDTR	2.28 (±1.42)	0.48 (±0.35)	3.17 (±2.16)	0.12 (±0.15)	1.51 (±1.81)	1.19
MDTWeQ	1.33 (±1.01)	0.21 (±0.21)	6.65 (±3.57)	0.13 (±0.0.25)	2.08 (±3.26)	1.57
MMPAWaQ	0.29 (±0.37)	0.21 (±0.24)	0.60 (±0.59)	0.09 (±0.16)	0.30 (±0.42)	1.41
PAWM	0.75 (±0.49)	0.36 (±0.31)	0.26 (±0.28)	0.05 (±0.13)	0.35 (±0.41)	1.17
PPMin	0.82 (±0.79)	0.40 (±0.60)	2.61 (±2.00)	0.39 (±0.89)	1.10 (±1.50)	1.42
PPRange	2.67 (±1.72)	1.07 (±1.18)	4.90 (±2.12)	0.75 (±0.55)	2.35 (±2.23)	0.95
PS	8.69 (±1.96)	1.93 (±1.09)	4.40 (±2.98)	2.42 (±1.13)	4.36 (±3.30)	0.76
TS	88.69 (±6.45)	2.55 (±3.05)	96.03 (±2.97)	24.78 (±5.87)	53.01 (±40.69)	0.77

b)

Predictors	Algorithms (n=25)				mean (n=100)	CV
	MaxEnt	RF	GLM	BRT		
Iso	0.72 (±0.76)	0.77 (±1.16)	4.19 (±1.58)	0.07 (±0.09)	1.44 (±1.92)	1.34
MDTR	4.24 (±1.21)	0.94 (±0.54)	0.31 (±0.23)	1.37 (±0.43)	1.72 (±1.67)	0.97
MDTWeQ	0.02 (±0.04)	0.09 (±0.07)	3.31 (±1.89)	0.10 (±0.11)	0.89 (±1.69)	1.92
MMPACQ	0.55 (±0.34)	0.18 (±0.15)	0.35 (±0.37)	0.09 (±0.13)	0.29 (±0.32)	1.08
MMPAWaQ	0.74 (±0.76)	0.16 (±0.23)	1.14 (±0.92)	0.04 (±0.08)	0.52 (±0.75)	1.44
PAWM	1.41 (±0.98)	0.20 (±0.16)	0.29 (±0.43)	0.09 (±0.10)	0.5 (±0.76)	1.53
PPMean	0.17 (±0.20)	0.26 (±0.22)	5.53 (±1.93)	0.06 (±0.08)	1.51 (±2.53)	1.68
PPRange	0.59 (±0.35)	0.33 (±0.36)	8.68 (±2.21)	0.16 (±0.17)	2.44 (±3.79)	1.55
PS	6.71 (±2.09)	0.96 (±0.42)	0.28 (±0.32)	2.64 (±1.07)	2.65 (±2.78)	1.05

TS	56.87 (±14.34)	3.18 (±2.06)	96.74 (±2.07)	17.66 (±6.90)	43.61 (±33.47)	0.86
VPDMin	3.28 (±1.42)	1.34 (±0.94)	14.31 (±3.30)	2.92 (±2.04)	5.46 (±5.59)	1.02
VPDRange	0.03 (±0.05)	0.41 (±0.25)	6.69 (±2.71)	0.59 (±0.45)	1.93 (±3.08)	1.60

c)

Predictors	**Algorithms (n=25)**				**mean (n=100)**	**CV**
	MaxEnt	**RF**	**GLM**	**BRT**		
Iso	1.44 (±1.01)	0,70 (±0.99)	0.15 (±0.13)	0.89 (±1.18)	0.80 (±1.02)	1.28
MMPACQ	0.90 (±1.00)	0.74 (±0.90)	5.45 (±2.43)	6.23 (±5.08)	3.33 (±3.82)	1.15
MMPAWaQ	0.05 (±0.09)	0.05 (±0.08)	1.90 (±1.32)	0.01 (±0.20)	0.50 (±1.04)	2.06
PADM	2.97 (±2.64)	1.63 (±1.38)	0.32 (±0.40)	3.18 (±2.31)	2.02 (±2.20)	1.08
PAWM	0.43 (±2.64)	0.17 (±0.25)	3.02 (±2.31)	0.05 (±0.10)	0.92 (±1.69)	1.84
PPMax	0.00 (±0.01)	0.67 (±0.64)	2.78 (±2.28)	2.46 (±1.12)	1.48 (±1.75)	1.18
PPRange	2.43 (±1.39)	0.36 (±0.43)	13.33 (±3.79)	0.48 (±0.52)	4.15 (±5.75)	1.39
VPDMean	13.14 (±4.34)	0.28 (±0.37)	63.54 (±6.28)	0.55 (±0.42)	19.38 (±26.42)	1.36
VPDRange	42.08 (±7.96)	0.58 (±0.48)	92.92 (±3.23)	1.13 (±0.63)	34.18 (±38.3)	1.12

d)

Predictors	**Algorithms (n=25)**				**mean (n=100)**	**CV**
	MaxEnt	**RF**	**GLM**	**BRT**		
Iso	30.89 (±6.17)	1.43 (±0.32)	0.26 (±0.24)	1.23 (±0.39)	8.45 (±13.38)	1.58
MDTDQ	0.41 (±0.42)	0.29 (±0.16)	38.63 (±4.70)	0.30 (±0.36)	9.91 (±16.83)	1.70
MDTR	2.65 (±0.50)	0.46 (±0.25)	0.13 (±0.13)	0.34 (±0.11)	0.9 (±1.07)	1.19
MDTWeQ	0.28 (±0.23)	0.20 (±0.13)	0.14 (±0.15)	0.12 (±0.06)	0.18 (±0.17)	0.90
MMPACQ	1.78 (±0.41)	0.61 (±0.21)	0.03 (±0.06)	0.59 (±0.48)	0.75 (±0.72)	0.96
PADM	1.40 (±0.44)	0.79 (±0.17)	0.89 (±0.24)	0.75 (±0.25)	0.96 (±0.39)	0.41
PAWM	3.85 (±0.66)	0.62 (±0.14)	0.67 (±0.22)	0.46 (±0.14)	1.40 (±1.47)	1.05
PPMin	0.70 (±0.44)	0.30 (±0.23)	9.00 (±0.79)	0.10 (±0.08)	2.53 (±3.79)	1.50
PPRange	0.99 (±0.29)	0.31 (±0.16)	3.60 (±0.50)	0.38 (±0.16)	1.32 (±1.38)	1.05
PS	1.18 (±0.27)	0.14 (±0.10)	3.61 (±0.68)	0.01 (±0.05)	1.24 (±1.49)	1.21
TS	0.24 (±0.17)	1.58 (±0.51)	73.90 (±3.47)	6.73 (±3.59)	20.61 (±31.11)	1.51
VPDMin	1.70 (±0.55)	0.13 (±0.09)	0.96 (±0.36)	0.05 (±0.06)	0.71 (±0.75)	1.05

e)

Predictors	**Algorithms (n=25)**				**mean (n=100)**	**CV**
	MaxEnt	**RF**	**GLM**	**BRT**		

MDTDQ	0.38 (±0.28)	0.38 (±0.20)	50.99 (±4.06)	0.26 (±0.19)	13.00 (±22.14)	1.70
MDTR	6.78 (±1.20)	0.39 (±0.15)	0.75 (±0.22)	0.16 (±0.07)	2.02 (±2.84)	1.40
MDTWeQ	0.72 (±0.21)	1.23 (±0.36)	17.75 (±2.68)	1.29 (±0.26)	5.25 (±7.38)	1.41
MMPACQ	5.14 (±0.71)	0.94 (±0.28)	0.23 (±0.13)	0.61 (±0.23)	1.73 (±2.03)	1.18
MMPAWaQ	0.33 (±0.47)	1.36 (±0.33)	0.31 (±0.19)	1.49 (±0.47)	0.87 (±0.67)	0.77
PADM	0.44 (±0.17)	0.40 (±0.11)	0.41 (±0.23)	0.03 (±0.05)	0.32 (±0.23)	0.72
PAWM	12.38 (±2.50)	0.90 (±0.30)	0.47 (±0.23)	7.93 (±1.36)	5.42 (±5.21)	0.96
PPMax	2.23 (±0.82)	0.39 (±0.12)	9.42 (±1.26)	0.18 (±0.09)	3.05 (±3.85)	1.26
PPMin	2.55 (±0.73)	1.03 (±0.19)	10.17 (±1.03)	1.10 (±0.27)	3.71 (±3.85)	1.04
VPDMin	44.42 (±3.83)	1.80 (±0.61)	23.30 (±4.76)	2.54 (±0.71)	18.02 (±17.87)	0.99
VPDRange	0.63 (±0.37)	0.97 (±0.24)	11.24 (±2.04)	0.83 (±0.21)	3.42 (±4.66)	1.36

f)

Predictors	**Algorithms (n=25)**				**mean (n=100)**	**CV**
	MaxEnt	**RF**	**GLM**	**BRT**		
APA	0.79 (±0.55)	0.36 (±0.24)	4.05 (±2.67)	0.04 (±0.07)	1.31 (±2.10)	1.60
Iso	9.53 (±3.30)	2.94 (±1.22)	62.00 (±13.50)	33.74 (±5.77	27.05 (±24.48)	0.90
MDTR	4.30 (±1.12)	2.60 (±0.79)	14.14 (±5.31)	5.74 (±1.50)	6.70 (±5.27)	0.79
MDTWeQ	0.50 (±0.73)	0.36 (±0.24)	27.40 (±11.30)	0.45 (±0.34)	7.18 (±12.99)	1.81
MMPACQ	3.46 (±1.18)	0.46 (±0.27)	0.19 (±0.30)	0.05 (±0.13)	1.04 (±1.54)	1.48
MMPAWaQ	0.42 (±0.38)	0.23 (±0.14)	1.68 (±0.93)	0.13 (±0.11)	0.61 (±0.80)	1.31
PADM	1.89 (±0.90)	0.17 (±0.13)	9.47 (±3.63)	0.15 (±0.17)	2.92 (±4.29)	1.47
PPMax	0.15 (±0.18)	1.00 (±0.46)	1.80 (±0.79)	1.92 (±0.71)	1.21 (±0.92)	0.76
PPMin	0.59 (±0.28)	0.27 (±0.22)	8.02 (±1.44)	0.04 (±0.06)	2.23 (±3.44)	1.54
PS	1.58 (±1.04)	1.48 (±0.71)	0.57 (±0.60)	1.91 (±0.86)	1.39 (±0.95)	0.69
VPDMin	8.92 (±3.26)	1.22 (±0.63)	1.91 (±1.84)	0.53 (±0.52)	3.15 (±3.88)	1.23
VPDRange	2.73 (±0.93)	0.18 (±0.14)	1.89 (±1.95)	0.05 (±0.07)	1.21 (±1.56)	1.29

g)

Predictors	**Algorithms (n=25)**				**mean (n=100)**	**CV**
	MaxEnt	**RF**	**GLM**	**BRT**		
MDTR	5.10 (±2.56)	1.27 (±1.43)	0.52 (±0.48)	2.37 (±1.97)	2.31 (±2.47)	1.07
MDTWeQ	0.79 (±1.37)	0.34 (±0.37)	0.82 (±0.86)	0.17 (±0.26)	0.53 (±0.88)	1.65
MMPACQ	0.98 (±1.05)	0.91 (±0.82)	0.69 (±0.47)	3.03 (±2.61)	1.40 (±1.74)	1.24
MMPAWaQ	4.19 (±2.17)	0.61 (±1.11)	12.06 (±6.41)	0.74 (±0.86)	4.40 (±5.78)	1.31

PADM	30.12 (±12.83)	1.21 (±1.57)	76.53 (±9.05)	1.00 (±1.06)	27.21 (±31.95)	1.17
PAWM	0.30 (±0.38)	0.48 (±0.47)	0.82 (±0.76)	0.37 (±0.50)	0.49 (±0.57)	1.16
PPMin	22.61 (±8.58)	3.37 (±4.75)	26.33 (±9.12)	25.47 (±7.88)	19.45 (±12.14)	0.62
PS	2.25 (±2.07)	1.10 (±1.01)	11.92 (±3.74)	2.42 (±1.52)	4.42 (±4.94)	1.12

h)

Predictors	**Algorithms (n=25)**				**mean (n=100)**	**CV**
	MaxEnt	**RF**	**GLM**	**BRT**		
Iso	7.79 (±1.24)	1.72 (±0.24)	0.72 (±0.22)	1.45 (±0.55)	2.92 (±2.93)	1.00
MDTR	7.10 (±0.69)	0.78 (±0.15)	0.08 (±0.09)	1.12 (±0.16)	2.27 (±2.85)	1.26
MDTWeQ	0.66 (±0.15)	0.89 (±0.22)	4.62 (±0.59)	1.40 (±0.20)	1.89 (±1.64)	0.87
MMPAWaQ	0.31 (±0.11)	0.42 (±0.13)	0.12 (±0.10)	0.07 (±0.09)	0.23 (±0.18)	0.78
PADM	0.32 (±0.08)	0.69 (±0.17)	0.86 (±0.30)	0.20 (±0.08)	0.52 (±0.32)	0.63
PAWM	5.83 (±0.53)	1.08 (±0.19)	0.01 (±0.03)	0.37 (±0.14)	1.82 (±2.37)	1.30
PPMin	1.24 (±0.23)	0.64 (±0.18)	10.90 (±0.60)	0.80 (±0.18)	3.40 (±4.37)	1.29
PPRange	1.54 (±0.23)	0.83 (±0.18)	4.89 (±0.35)	1.66 (±0.26)	2.23 (±1.60)	0.72
PS	3.51 (±0.42)	0.49 (±0.12)	4.42 (±0.57)	0.20 (±0.09)	2.15 (±1.88)	0.87
TS	1.02 (±0.34)	4.52 (±0.64)	99.89 (±0.14)	32.70 (±1.19)	34.53 (±39.89)	1.16
VPDMin	9.86 (±2.13)	0.89 (±0.19)	7.09 (±0.57)	0.07 (±0.07)	4.48 (±4.29)	0.96
VPDRange	0.59 (±0.18)	0.24 (±0.09)	2.56 (±0.31)	0.00 (±0.00)	0.85 (±1.03)	1.21

Table 1.6. Calculated areas of the classes of suitability for the various algorithms (BRT, GLM, MaxEnt and RF) and for *A. barreirensis*, *A. eichleri*, *A. funifera*, *A. maripa*, *A. phalerata*, *A. speciosa*, *A. vitrivir*, and the Babassu Complex overall in the current scenario.

Species	Class	Algorithms (km²)				Ensemble map (km²)
		BRT	GLM	MaxEnt	RF	
A. barreirensis	Unsuitable	13634187	12969299	10905077	14058727	11912656
	Low	6213786	3856431	6055359	5309672	6464969
	Medium	1713127	2580292	3623780	1703246	2961686
	High	1363	2156442	978248	490818	254882
A. eichleri	Unsuitable	12429280	10206745	11682964	13369467	10189062
	Low	7518369	6255746	5409039	5697229	8416218
	Medium	1593143	3680293	3523524	1696250	2644049
	High	21671	1419680	946936	799517	344864
A. funifera	Unsuitable	11330256	17256849	14280289	14379435	14020352
	Low	10076050	2807763	6433105	6317610	7120495
	Medium	145691	773799	771506	802808	422180
	High	10467	724053	77564	62611	31166
A. maripa	Unsuitable	11967586	12243827	12177871	12459396	11817501
	Low	5954938	3499207	3760769	5199122	4637818
	Medium	3639939	2235268	4048532	2897280	4223378
	High	0	3584161	1575292	1006666	915496
A. phalerata	Unsuitable	7539385	9470269	8345042	9922433	7759199
	Low	11696008	6690289	7223609	8226021	9935641
	Medium	2327070	4056093	4044635	2160187	3165997
	High	0	1345813	1949178	1253823	733356
A. speciosa	Unsuitable	11886372	9869652	9311258	10663904	9460532
	Low	5258244	5449361	5269999	6203454	6585918
	Medium	4414489	4157888	5026396	3049355	4620239
	High	3359	2085563	1954811	1645751	927503
A. vitrivir	Unsuitable	9945873	17772173	14418881	15714232	14502398
	Low	11281382	2331444	5012342	4676827	5819594
	Medium	335209	970969	1715391	907519	1086344

	High	0	487877	415851	263885	185856
Babassu Complex	Unsuitable	7518791	7668912	7853995	8309833	7467461
	Low	8231298	5219682	3573677	7340167	5808119
	Medium	5812375	6284256	6498762	4849699	7891228
	High	0	2389614	3636030	1062765	427386

Table S1.7. The total sum of the areas of the whole species for each of the classes of suitability for the various algorithms (BRT, GLM, MaxEnt and RF) in the current scenario.

Class	Algorithms (km²)			
	BRT	GLM	MaxEnt	RF
Unsuitable	86251730.71	97457726.66	88975378.68	98877426.89
Low	66230075.32	36109923.49	42737898.39	48970102.14
Medium	19981044.06	24738857.10	29252525.03	18066344.11
High	36859.92	14193202.77	11533907.91	6585836.88

a) *Attalea barreirensis*

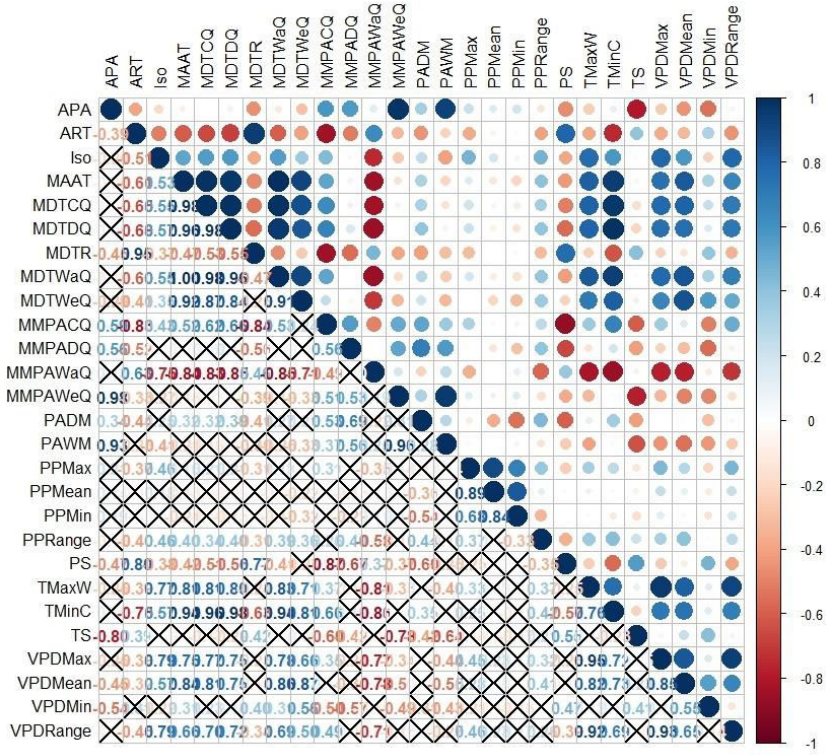

b) *Attalea eichleri*

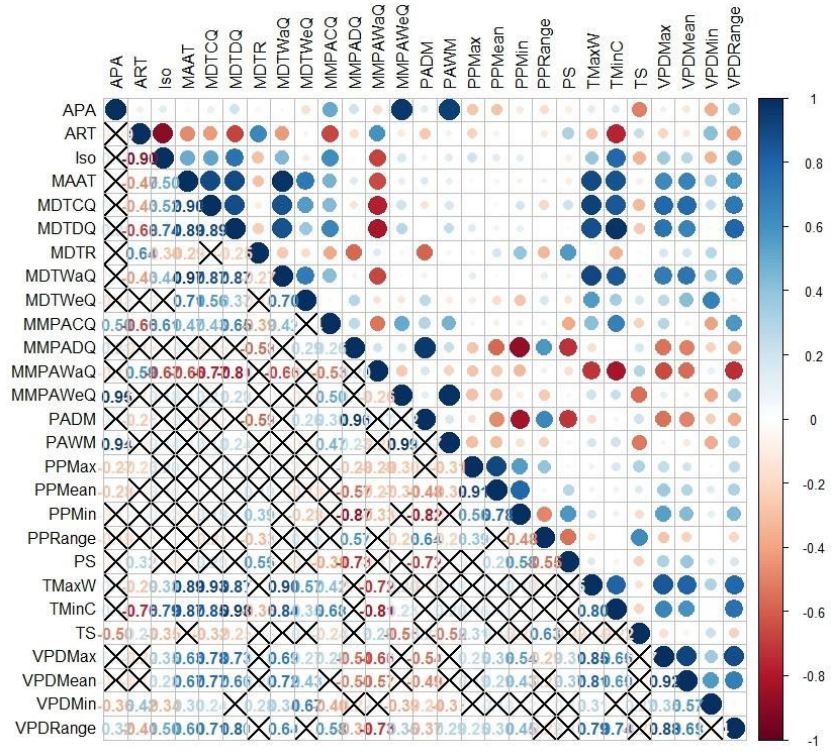

c) *Attalea funifera*

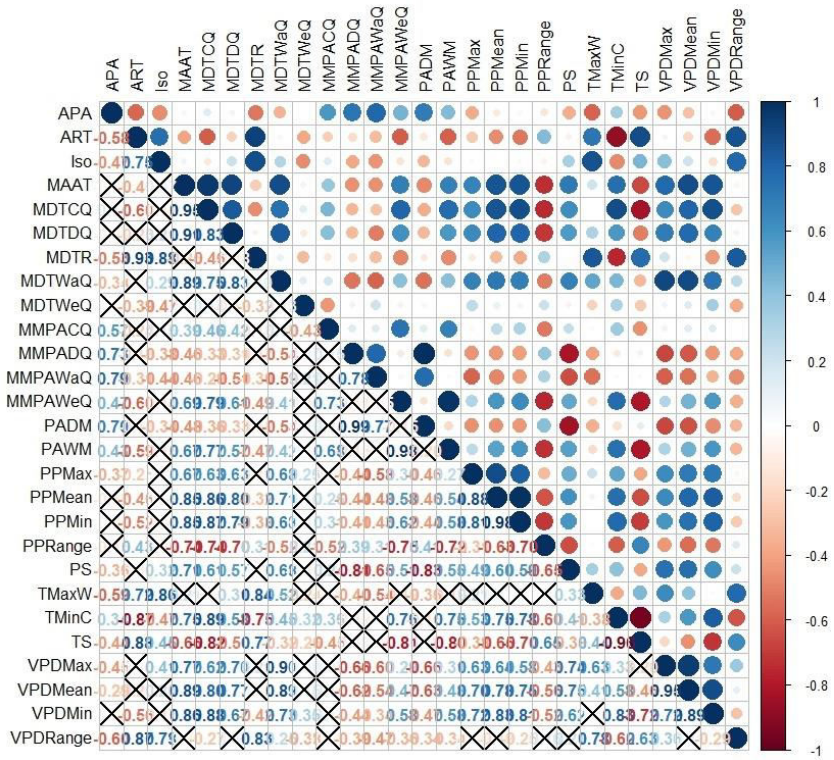

d) *Attalea maripa*

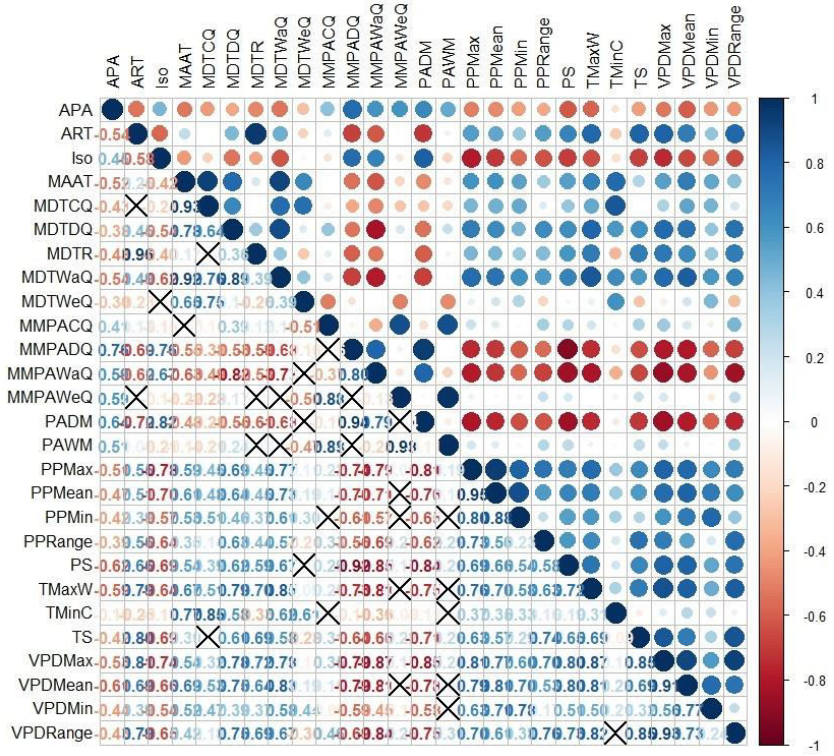

e) *Attalea phalerata*

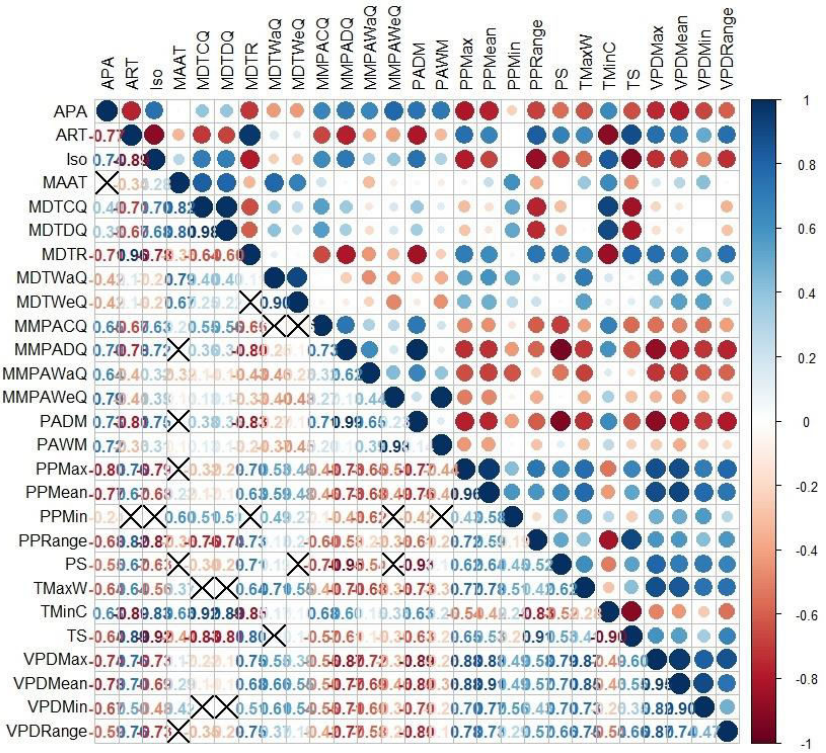

f) *Attalea speciosa*

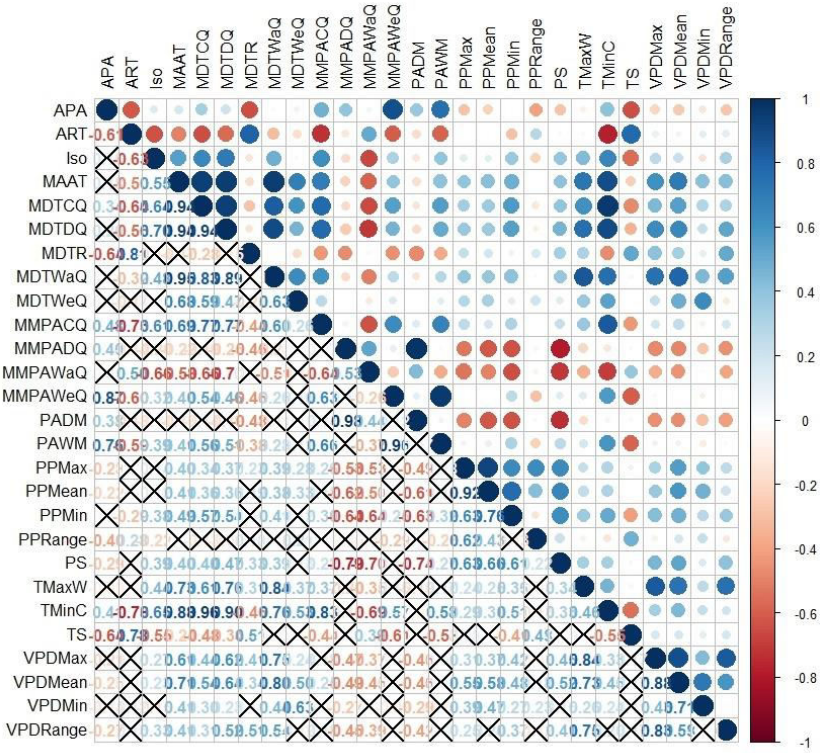

g) *Attalea vitrivir*

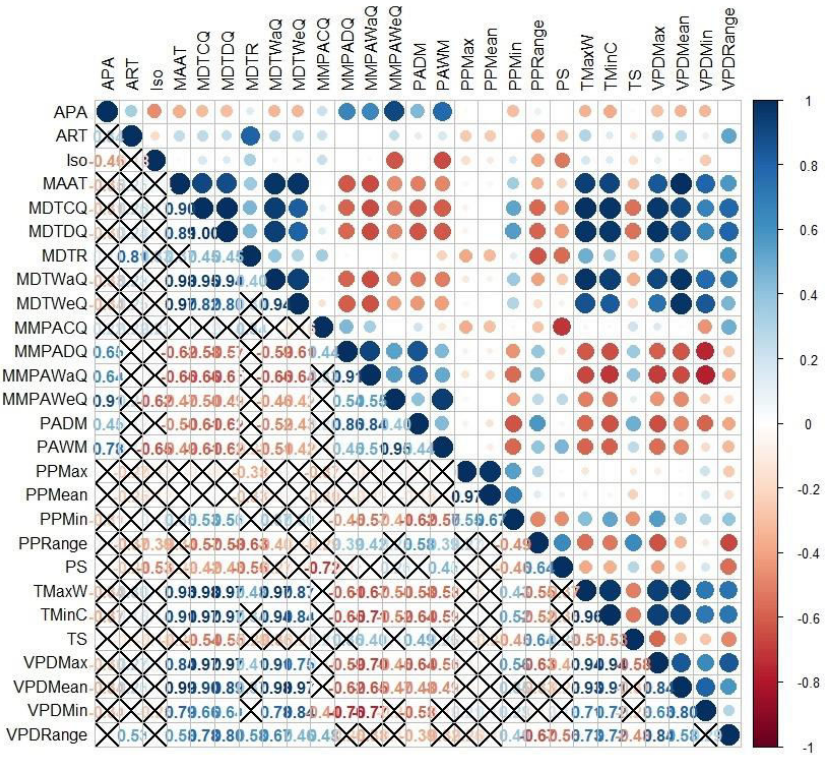

h)

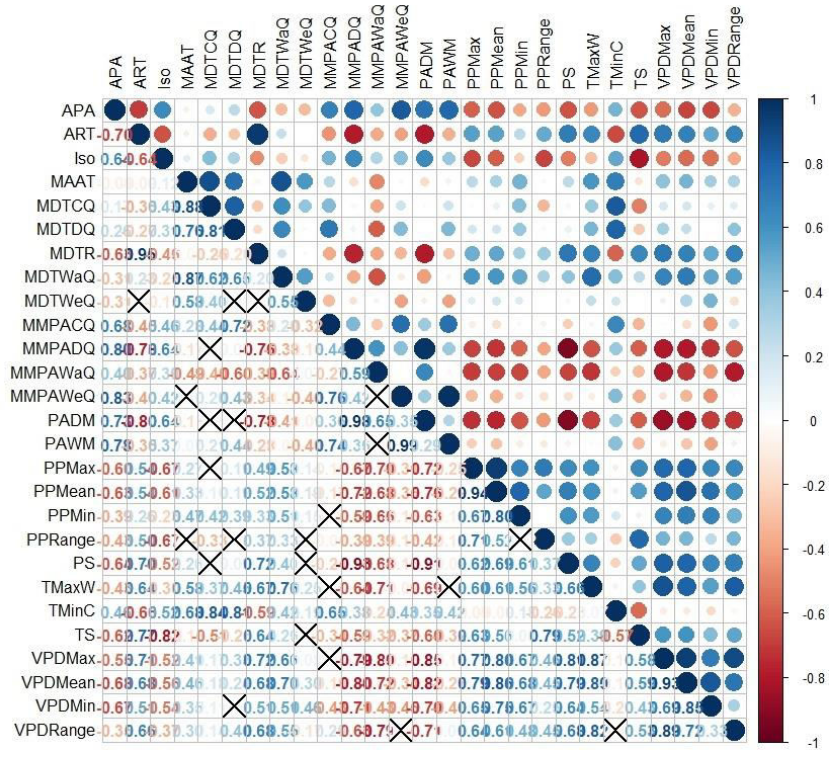

Figure S1.1. Spearman's correlation test for the set of bioclimatic variables for a) *A. barreirensis* (n = 41), b) *A. eichleri* (n = 79), c) *A. funifera* (n = 65), d) *A. maripa* (n = 570), e) *A. phalerata* (n = 431), f) *A. speciosa* (n = 84), g) *A. vitrivir* (n = 27), and h) the Babassu Complex overall (n = 1,269). Marked cells represent non-significant correlations at $p \leq 0.05$.

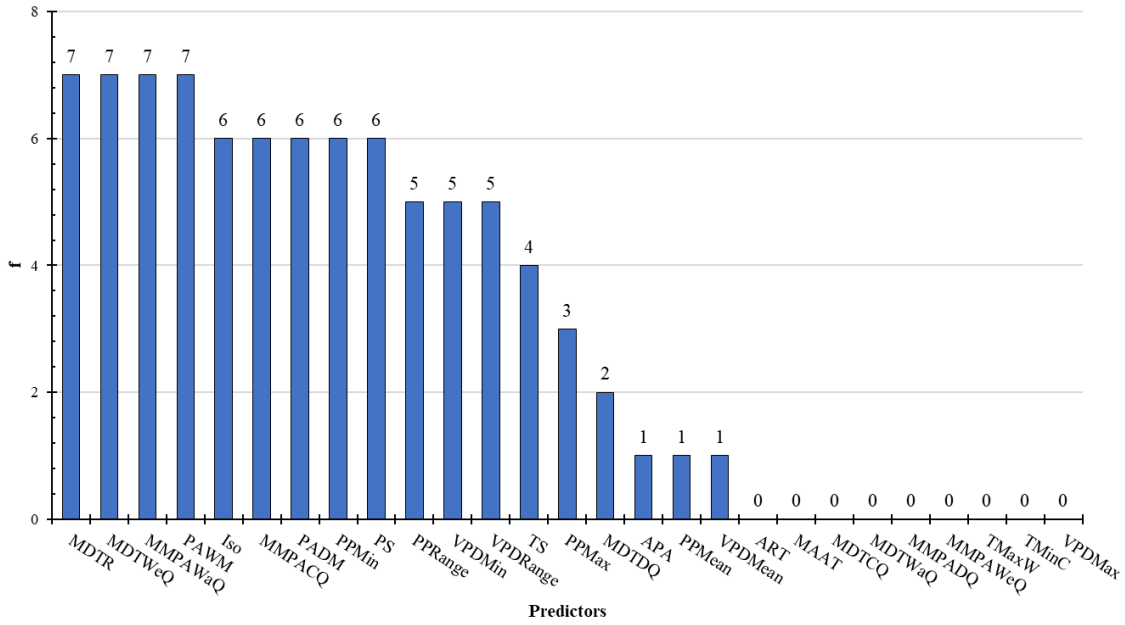

Figure S1.2. Frequency (f) of the remaining bioclimatic variables used for fitting current scenario models after multicollinearity analysis, considering all individual species and the Babassu Complex overall.

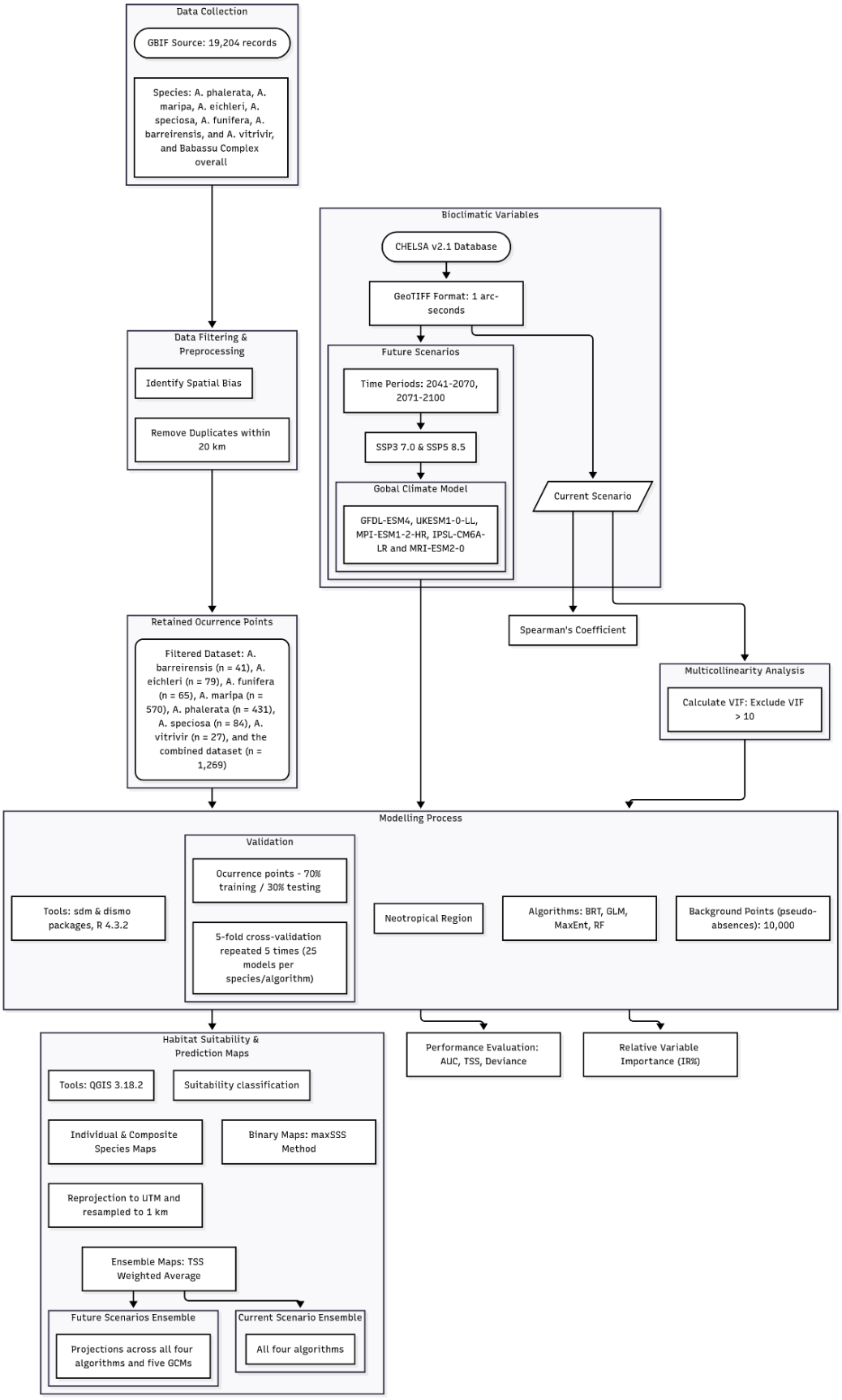

Figure S1.3. Methodological workflow for the species distribution modelling of the Babassu Complex and its species.

a) *A. barreirensis*

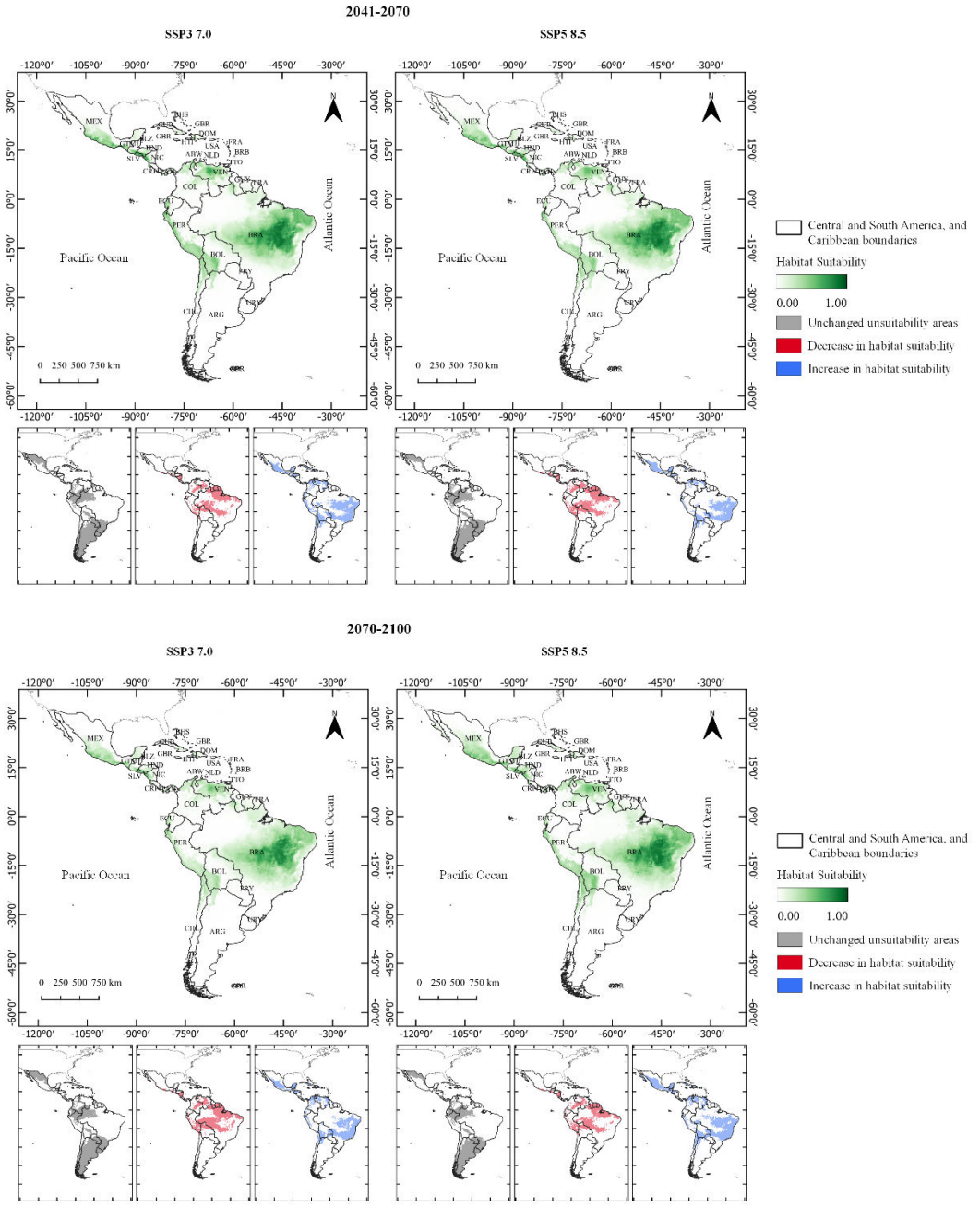

b) *A. eichleri*

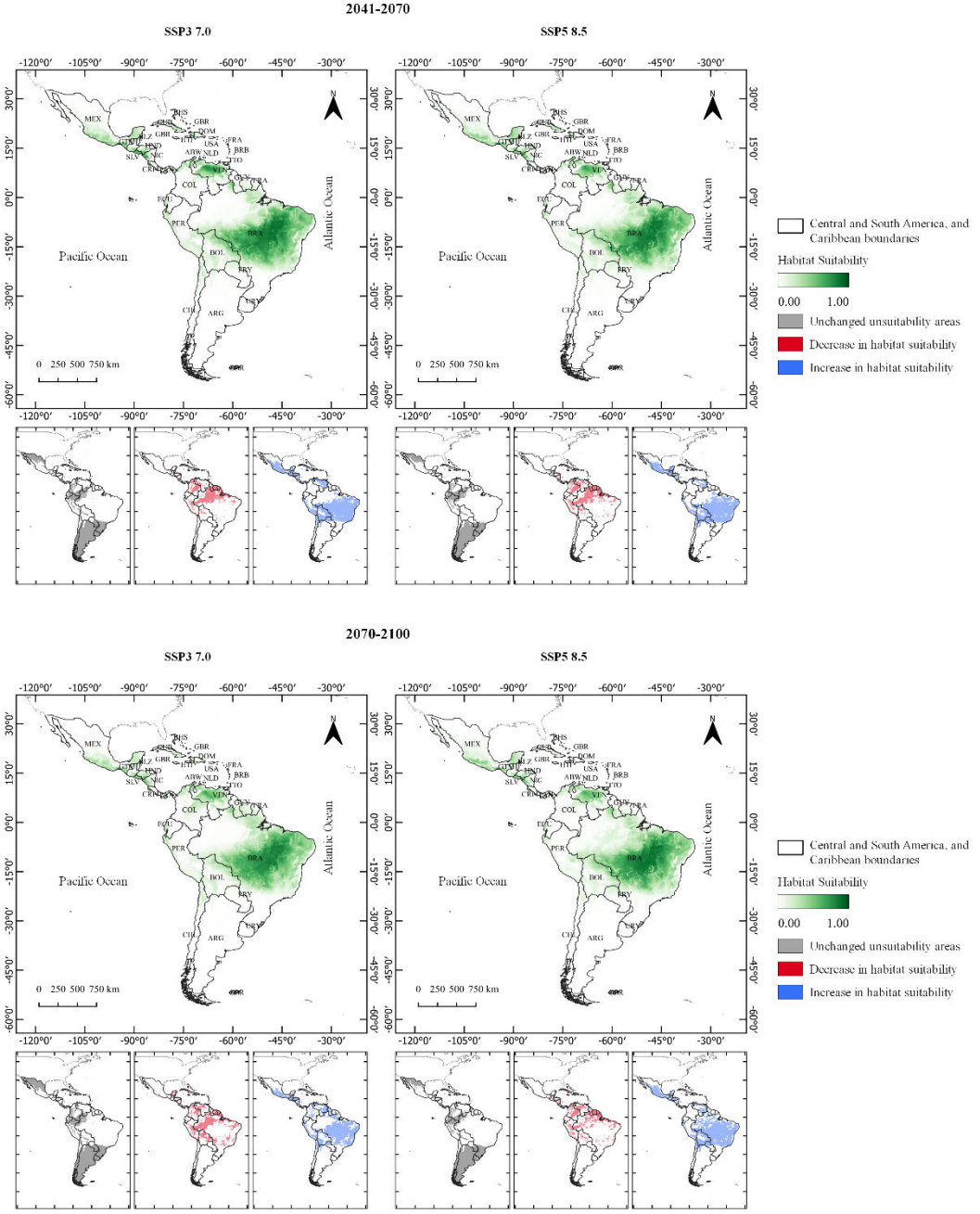
2041-2070
SSP3 7.0
SSP5 8.5
Pacific Ocean
Atlantic Ocean
0 250 500 750 km
Central and South America, and Caribbean boundaries
Habitat Suitability
0.00 1.00
Unchanged unsuitability areas
Decrease in habitat suitability
Increase in habitat suitability
2070-2100
SSP3 7.0
SSP5 8.5
Pacific Ocean
Atlantic Ocean
0 250 500 750 km
Central and South America, and Caribbean boundaries
Habitat Suitability
0.00 1.00
Unchanged unsuitability areas
Decrease in habitat suitability
Increase in habitat suitability

c) *A. funifera*

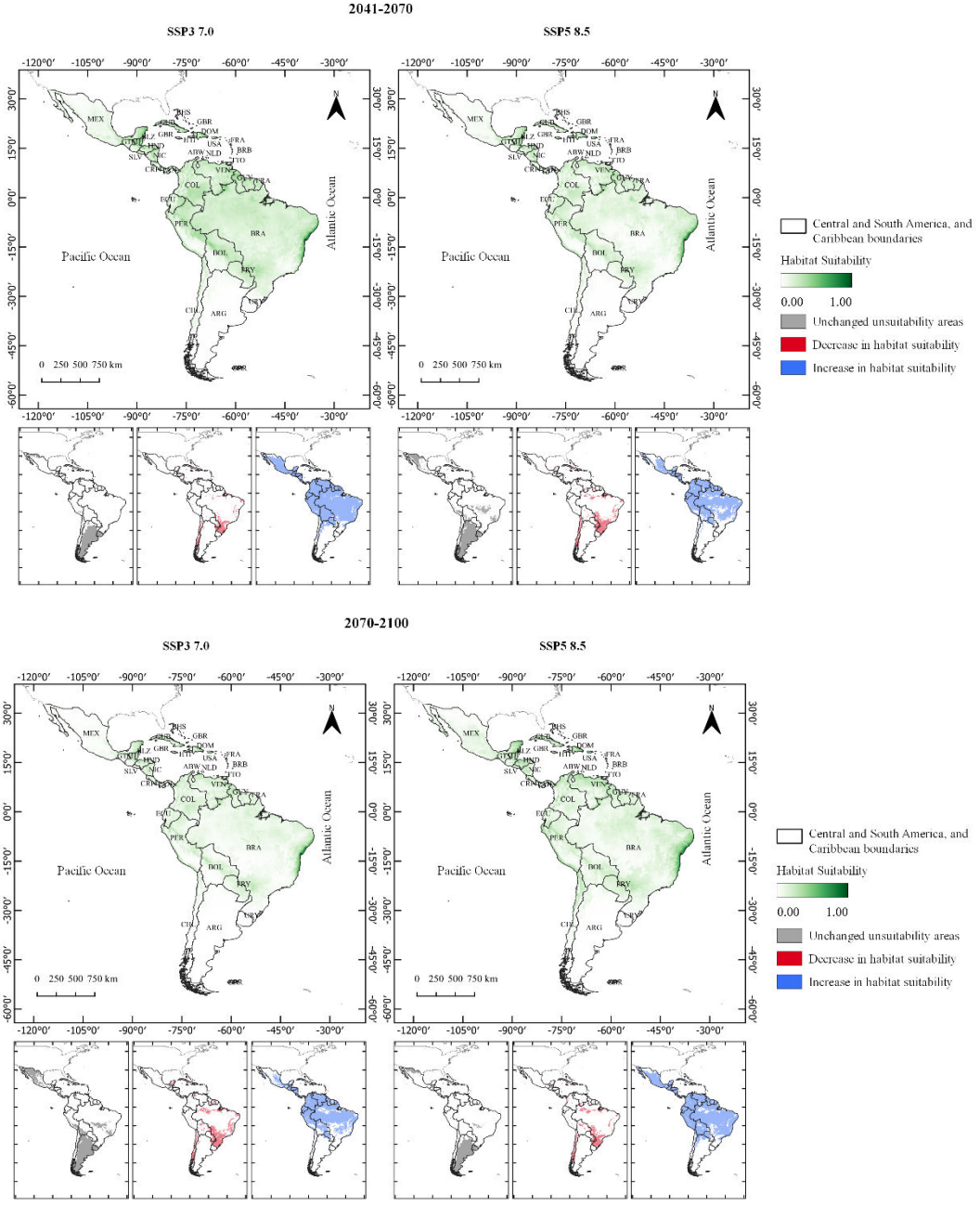
2041-2070
SSP3 7.0
SSP5 8.5
Pacific Ocean
Atlantic Ocean
0 250 500 750 km
Central and South America, and Caribbean boundaries
Habitat Suitability
0.00 1.00
Unchanged unsuitability areas
Decrease in habitat suitability
Increase in habitat suitability
2070-2100
SSP3 7.0
SSP5 8.5
Pacific Ocean
Atlantic Ocean
0 250 500 750 km
Central and South America, and Caribbean boundaries
Habitat Suitability
0.00 1.00
Unchanged unsuitability areas
Decrease in habitat suitability
Increase in habitat suitability

d) *A. maripa*

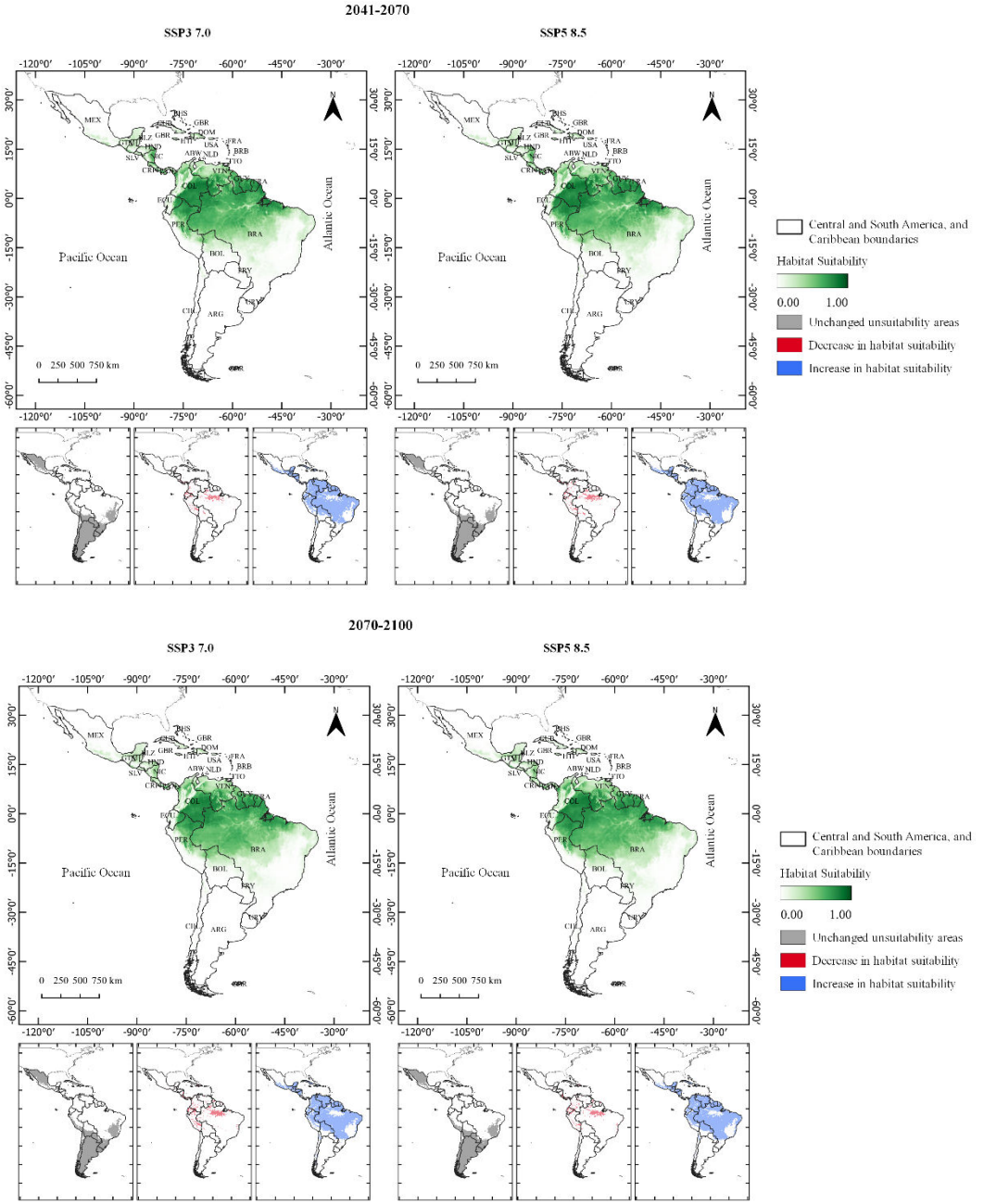
2041-2070
SSP3 7.0
SSP5 8.5
Pacific Ocean
Atlantic Ocean
0 250 500 750 km
2070-2100
SSP3 7.0
SSP5 8.5
Pacific Ocean
Atlantic Ocean
0 250 500 750 km
Central and South America, and Caribbean boundaries
Habitat Suitability
0.00 1.00
Unchanged unsuitability areas
Decrease in habitat suitability
Increase in habitat suitability

e) *A. phalerata*

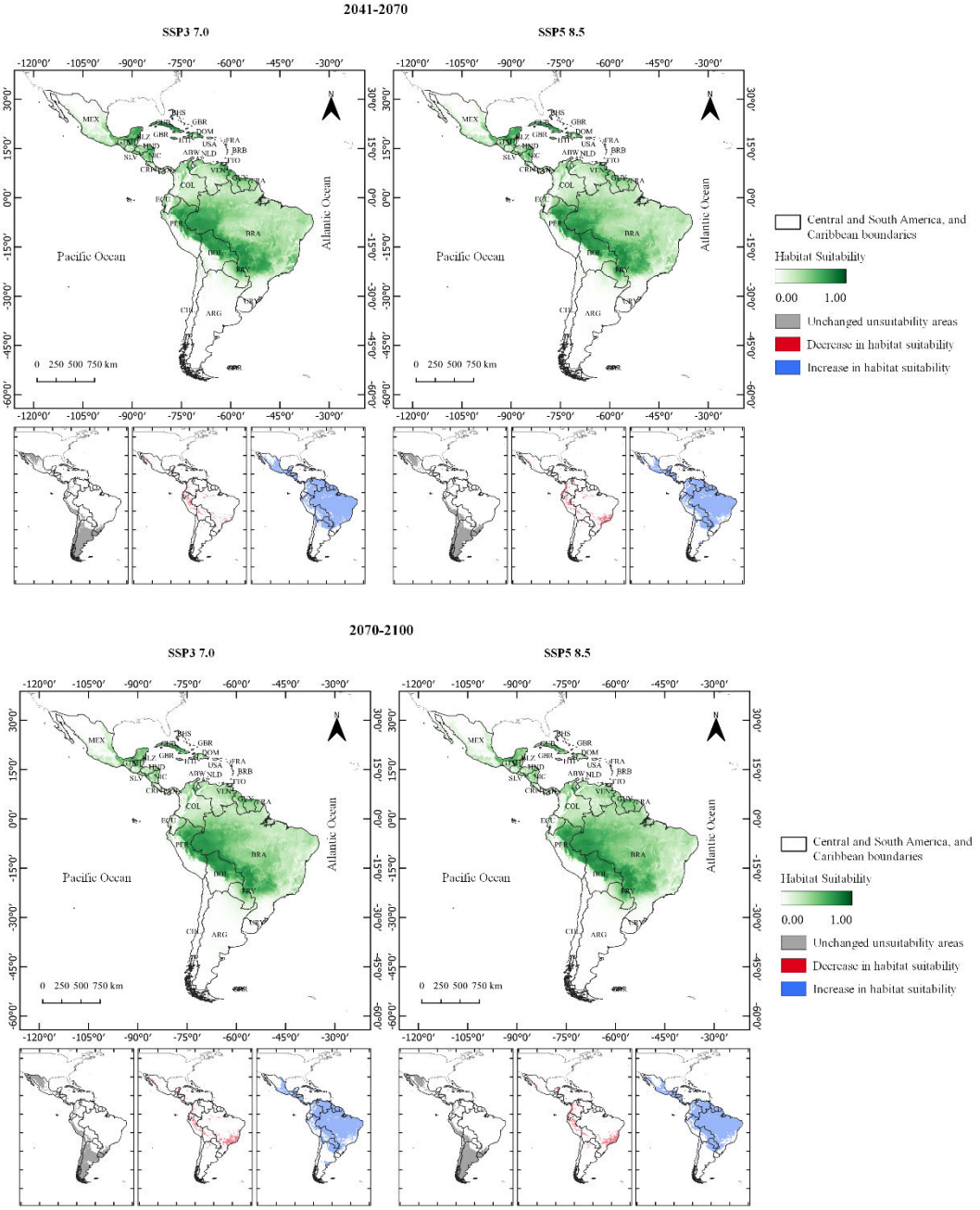

f) *A. speciosa*

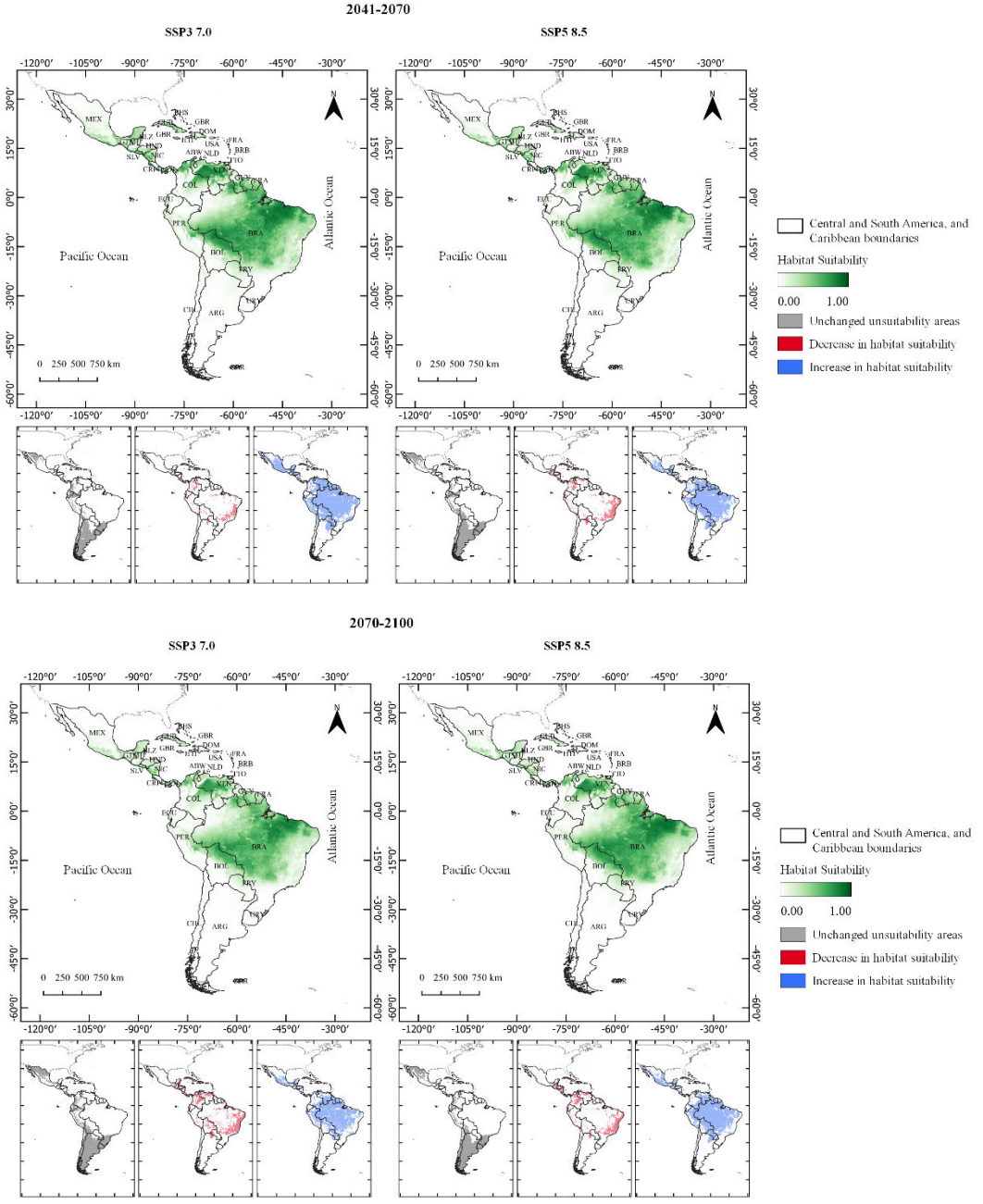
2041-2070
SSP3 7.0
SSP5 8.5
Pacific Ocean
Atlantic Ocean
0 250 500 750 km
Central and South America, and Caribbean boundaries
Habitat Suitability
0.00 1.00
Unchanged unsuitability areas
Decrease in habitat suitability
Increase in habitat suitability
2070-2100
SSP3 7.0
SSP5 8.5
Pacific Ocean
Atlantic Ocean
0 250 500 750 km
Central and South America, and Caribbean boundaries
Habitat Suitability
0.00 1.00
Unchanged unsuitability areas
Decrease in habitat suitability
Increase in habitat suitability

g) *A. vitrivir*

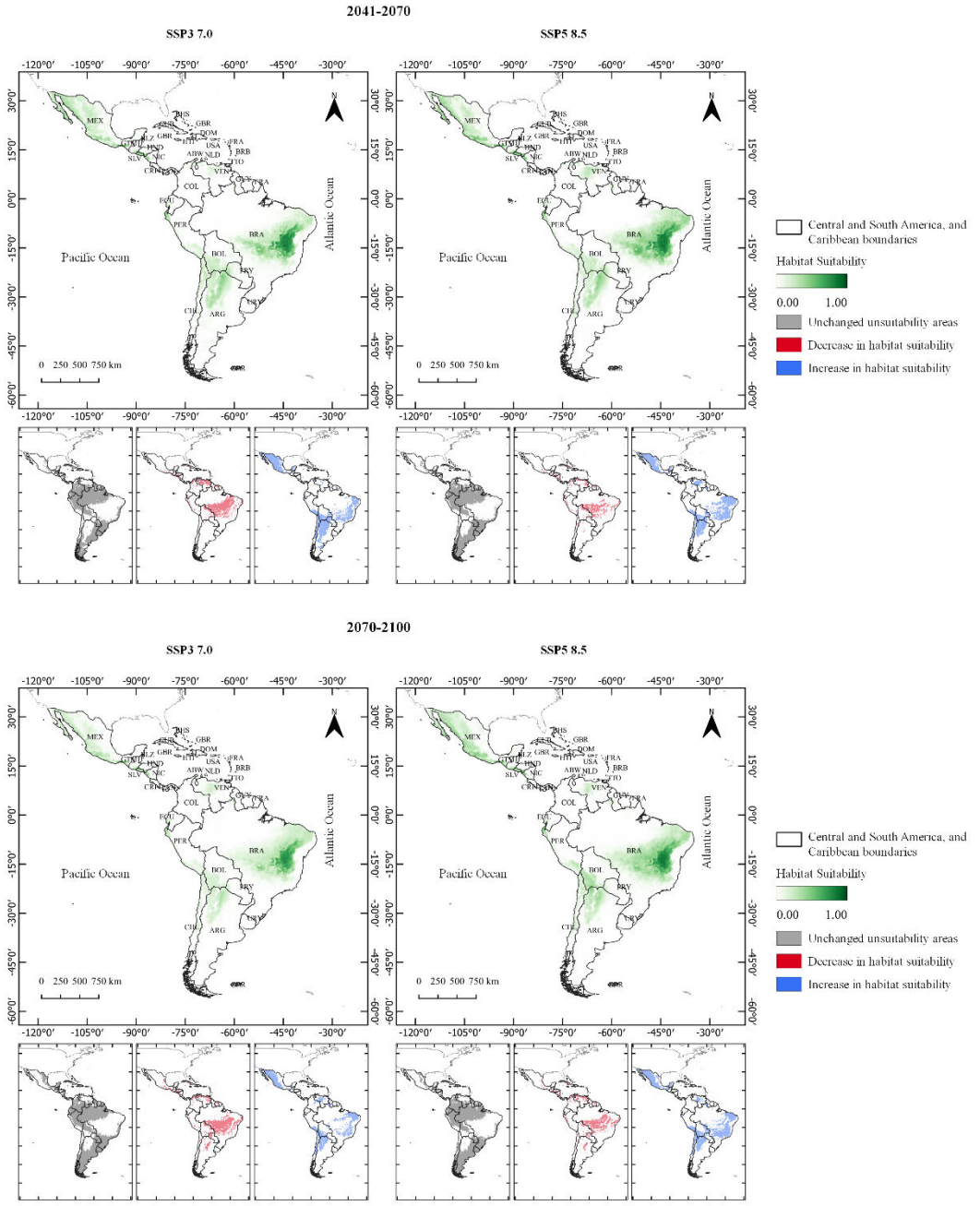
2041-2070
SSP3 7.0
SSP5 8.5
Pacific Ocean
Atlantic Ocean
0 250 500 750 km
2070-2100
SSP3 7.0
SSP5 8.5
Pacific Ocean
Atlantic Ocean
0 250 500 750 km
Central and South America, and Caribbean boundaries
Habitat Suitability
0.00 1.00
Unchanged unsuitability areas
Decrease in habitat suitability
Increase in habitat suitability

h) Babassu Complex overall

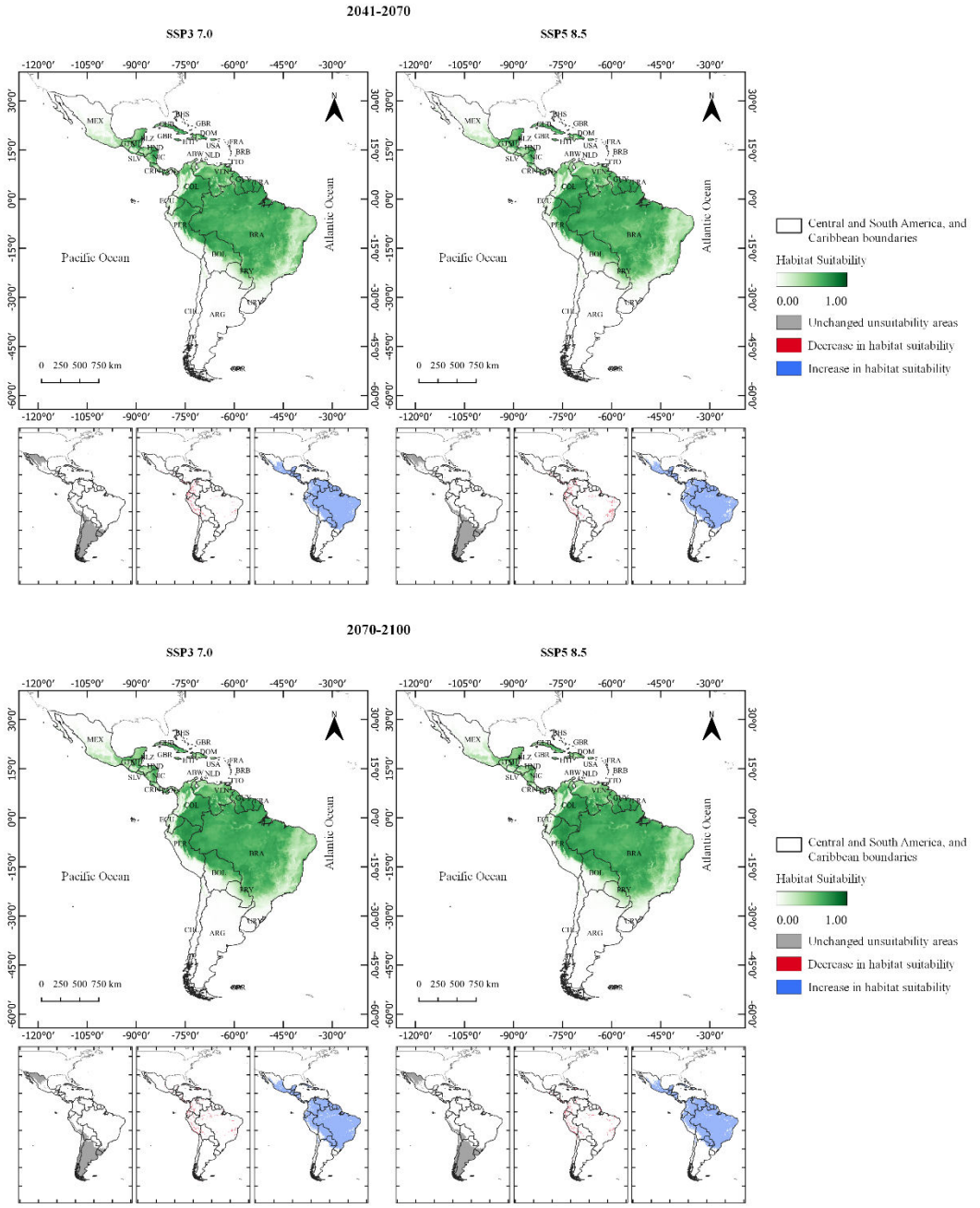

Figure S1.4. Ensemble of future projections habitat suitability and changes under SSP3 7.0 and SSP5 8.5 Scenarios (2041-2070 and 2070-2100) for a) *A. barreirensis*, b) *A. eichleri*, c) *A. funifera*, d) *A. maripa*, e) *A. phalerata*, f) *A. speciosa*, g) *A. vitrivir*, and h) the Babassu Complex overall, in Neotropical region.